Ⅲ　研究成果の刊行物・別冊

ACADEMIC PRESS

Available online at www.sciencedirect.com

SCIENCE DIRECT®

Biochemical and Biophysical Research Communications 299 (2002) 410–417

BBRC

www.academicpress.com

ABCC13, an unusual truncated ABC transporter, is highly expressed in fetal human liver☆,☆☆

Hikaru Yabuuchi,[a] Shin-ichiro Takayanagi,[a] Keigo Yoshinaga,[b] Naoyuki Taniguchi,[c] Hiroyuki Aburatani,[d] and Toshihisa Ishikawa[a,*]

[a] *Department of Biomolecular Engineering, Graduate School of Bioscience and Biotechnology, Tokyo Institute of Technology, 4259 Nagatsuta, Midori-ku, Yokohama 226-8501, Japan*

[b] *Second Department of Surgery, Tokyo Medical and Dental University, 1-5-45 Yushima, Bunkyo-ku, Tokyo 113-8519, Japan*

[c] *Department of Biochemistry and Molecular Biology, Graduate School of Medicine, Osaka University Medical School, 2-2 Yamadaoka, Suita, Osaka 565-0871, Japan*

[d] *Genome Science Division, Research Center for Advanced Science and Technology, The University of Tokyo, 4-6-1 Komaba, Meguro-ku, Tokyo 153-8904, Japan*

Received 24 October 2002

Abstract

In the present study, we have cloned the cDNA of ABCC13, a novel ABC transporter, from the cDNA library of adult human placenta. The *ABCC13* gene spans ~70 kb on human chromosome 21q11.2 and consists of 14 exons. The open reading frame of the ABCC13 cDNA encodes a peptide consisting of 325 amino acid residues. The amino acid sequence corresponding to putative membrane-spanning domains was remarkably similar to ABCC1, ABCC2, ABCC3, and ABCC6. The *ABCC13* gene was expressed in the fetal liver at the highest level among the organs studied. While ABCC13 was expressed in the bone marrow, its expression in peripheral blood leukocytes of adult humans was much lower and no detectable levels were observed in differentiated hematopoietic cells. The expression of ABCC13 in K562 cells decreased during cell differentiation induced by TPA. These results suggest that the expression of human ABCC13 is related with hematopoiesis.

Keywords: ABC transporter; Human chromosome 21; Fetal liver; Hematopoiesis; Leukemia cells; Cell differentiation

The ATP-binding cassette (ABC) transporters form one of the largest protein families and play a biologically important role as membrane transporters or ion channel modulators [1]. According to the recently published draft sequence of the human genome, more than 50 of human ABC transporter genes (including pseudogenes) are anticipated to exist in the human genome. Hitherto 48 human ABC-transporter genes have been identified and sequenced (recent reviews: [2–5]). Based on the arrangement of molecular structure components, i.e., the nucleotide binding domain and the topology of transmembrane-spanning domains, human ABC transporters are classified into seven sub-families from A to G (the new nomenclature of human ABC transporter genes: http://gene.ucl.ac.uk/nomenclature/genefamily/abc.html). Mutations of human ABC transporter genes have been reported to be the cause of genetic diseases, such as Tangier disease [6–8], cystic fibrosis [9], Dubin–Johnson syndrome [10], Stargardt disease [11], and sitosterolemia [12].

According to the new nomenclature of human ABC transporter genes, the ABCC gene family comprises the members of multidrug resistance-associated proteins (MRPs) [13], sulfonylurea receptors (SUR) [14], and cystic fibrosis transmembrane conductance regulator (CFTR) [9]. We have provided first evidence that

☆ *Abbreviations:* ABC, ATP-binding cassette; FCS, fetal calf serum, PCR, polymerase chain reaction; GS-X pump, ATP-dependent glutathione *S*-conjugate export pump; MRP, multidrug resistance-associated protein; PKC, paroxysmal kinesigenic choreoathetosis; TM, transmembrane; TPA, 12-*O*-tetradecanoyl phorbol-13-acetate.

☆☆ The sequence of ABCC13 cDNA has been registered in GenBank under Accession No. of AF418600 on September 7, 2001.

* Corresponding author. Fax: +81-45-924-5838.
E-mail address: tishikaw@bio.titech.ac.jp (T. Ishikawa).

0006-291X/02/$ - see front matter © 2002 Elsevier Science (USA). All rights reserved.
PII: S0006-291X(02)02658-X

transport of leukotriene C_4 (LTC_4), a pro-inflammatory mediator, across the cell membrane is mediated by a glutathione *S*-conjugate export pump (GS-X pump) [15–19]. Following studies have proven that the GS-X pump(s) is encoded by ABCC1 (MRP1) and ABCC2 (cMOAT or MRP2) genes [20–22]. ABCC1 (MRP1) and ABCC2 (cMOAT/MRP2) were identified by molecular cloning of cDNA from human multidrug resistant lung cancer cells [23] and from hepatobiliary transport mutant (TR^-) rats [22], respectively. After the discovery of the ABCC1 and ABCC2 genes, five human homologues, i.e., ABCC3 (MRP3), ABCC4 (MRP4), ABCC5 (MRP5), ABCC6 (MRP6), and ABCC10 (MRP7), have been successively identified. Those ABC transporters exhibit a wide spectrum of biological functions and are involved in transport of drugs as well as endogenous substances (see [2–5] for recent reviews).

Most recently, our group [24] and others [25–27] have independently discovered two novel ABC transporters, i.e., human ABCC11 (MRP8) and ABCC12 (MRP9), that belong to the ABCC sub-family. These genes consist of at least 30 and 29 exons, respectively, and they are tandemly located in a tail-to-head orientation on human chromosome 16q12.1 [24,25]. Recent linkage analyses have demonstrated that a putative gene responsible for paroxysmal kinesigenic choreoathetosis (PKC), a genetic disease of infancy, is located in the region of 16p11.2–q12.1 [28,29]. Since ABCC11 and ABCC12 genes are encoded at that 16q12.1 locus, a potential link between the PKC gene and these ABC transporters has been implicated.

In the present study, we have discovered another new ABCC transporter gene, named ABCC13, on the human chromosome 21 and cloned its cDNA from human placenta cDNA library. We herein describe the gene structure of ABCC13 and its expression profile in different organs and cell types. The highest expression of ABCC13 was detected in the fetal liver among different organs from fetal and adult humans. On the other hand, the expression of ABCC13 in leukemia K562 cells was down-regulated during cell differentiation.

Materials and methods

Cloning of cDNA encoding human ABCC13. The draft sequence of the human chromosome 21 (GenBank Accession No. AF130358) was analyzed by using the GENSCAN program (http://genes.mit.edu/GENSCAN.html) to predict the potential exons of ABCC13. EST clones were extracted from the currently available EST database to find partial sequences of the ABCC13 transcript.

To clone the ABCC13 cDNA, we have first screened the human placenta Master Plate of Rapid-Screen Arrayed cDNA Library Panel (OriGene, Rockville, MD, USA) by means of PCR using the following primers: the forward primer (hC13F): 5′-CATATTCCTGGTTTAGC AGA-3′ and the backward primer (hC13B): 5′-GTGAGCATGTTA AAACGTTG-3′). The PCR was performed with *Ex Taq* polymerase (TaKaRa, Japan), where the reaction consisted of 30 cycles of 95 °C for 30 s, 56 °C for 30 s, 72 °C for 30 s, and 72 °C for 2 min. The resulting PCR products were subjected to 1.2%-agarose gel electrophoresis to identify positive wells. The sub-plate corresponding to the positive wells on the Master Plate was analyzed by 96-well PCR under the same experimental conditions. Pre-transformed *Escherichia coli* cells in the positive wells were taken and plated on the LB amp plates. PCR was subsequently performed on 96 individual colonies using the same primers as described above. Positive colonies were isolated and pCMV6-XL4 plasmids containing ABCC13 cDNA were extracted using the QIAprep Spin Miniprep Kit (Qiagen GmbH, Germany). The sequence of the cloned ABCC13 cDNA was analyzed by automated DNA sequencing (TOYOBO Gene Analysis, Japan). The cDNA sequence of ABCC13, thus obtained, has been deposited to GenBank under Accession No. AF418600.

Data analysis. DNA sequences were analyzed with the GENETYX-MAC software ver.11 (Software Development, Japan) and compared with other ABCC transporter genes registered in the NCBI database. The hydropathy profile of the protein deduced from the cDNA sequence was calculated with the Kyte and Doolittle hydropathy algorithm [30], and transmembrane domains were predicted by using the SOSUI program (http://sosui.proteome.bio.tuat.ac.jp/sosuimenu0.html).

Cell culture and induction of cell differentiation. Human leukemia K562 cells were maintained to grow in RPMI 1640 supplemented with 10% heat-inactivated FCS and penicillin (100 U/ml) and streptomycin (100 μg/ml) in a humidified chamber (37 °C, 5% CO_2). The number of cells was determined in a hemocytometer by trypan blue dye exclusion. Differentiation of K562 cells (2×10^5 cells/ml) was induced by incubation with TPA at a final concentration of 10 nM for 4 days. Cell differentiation was monitored by the observation of morphological changes and the cell proliferation rate. At different incubation times, cells were withdrawn and total RNA was extracted as described below.

RNA extraction and preparation of cDNA. Total RNA was extracted from cultured cells using the ISOGEN RNA extraction solution (WAKO Pure Chemical Industries, Japan) according to manufacturer's protocol. cDNA was prepared from the extracted RNA in the reverse transcriptase reaction using Superscript II RT (Invitrogen, Gaithersburg, MD, USA) and oligo(dT) primers according to manufacturer's instruction.

Quantitative PCR analysis. Quantitative PCR was performed using cDNA from several cell lines and human tissues as well as Multiple Tissue cDNA (MTC) Panels (Clontech, Palo Alto, CA, USA). Two μl of each human cDNA was used for each 25 μl of the Ex Taq R-PCR Version (TaKaRa, Japan). The above-mentioned ABCC13-specific primers, i.e., hC13F and hC13B, were used for the quantitative PCR analysis. Each primer was used at a final concentration of 300 nM in the reaction mixture. Quantitative PCR analysis was performed using a Smart Cycler system (TaKaRa, Japan) with SYBR Green I (Bio-Whittaker Molecular Applications, Rockland, ME, USA) as a fluorescence indicator. The PCR consisted of 40 cycles of 95 °C for 15 s, 58 °C for 15 s, 72 °C for 15 s, and 85 °C for 7 s. The resulting PCR product was a 442-bp fragment. The expression levels of ABCC13 were normalized with β-actin mRNA levels. For this purpose, PCR was carried out to detect β-actin expression by using the following primers: the forward primer, TGAAGTACCCCATCGAGCACG and the backward primer, CAAACATGATCTGGGTCATCTTCTC. The PCR consisted of 40 cycles of 95 °C for 15 s, 58 °C for 15 s, 72 °C for 15 s, and 90 °C for 7 s. The resulting PCR product was 174-bp long.

Results and discussion

Gene structure of human ABCC13

A novel ABCC transporter gene, *ABCC13*, was discovered by database search on the human chromosome

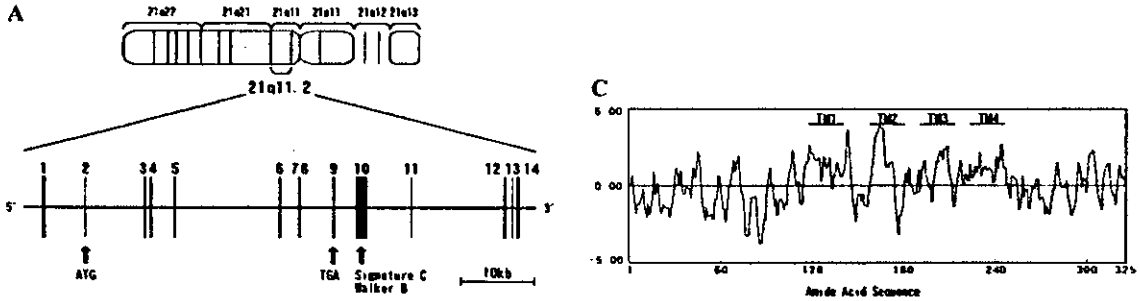

B

```
ttcccgtctccctccacaccttgcctcctccaggcccaaccccattccaccagcaccc:gccccaggcgcactggctaggactggaaggcaaggactaaggtgaaagctgactgcccgca  120
ccgccccaggcgcactgggtaggactgaaaggcaggggactaaggtgacagctgactctgccgggcggagtgcgtgtcctcccaccgtgctggcgctgaactgactgtccgctgccaagg  240
gaagtgacagccgcagccgggctctcagccagcggccgggcgccccagcggaccATGCTCTCCAGTACGCAGAACGCGGGCGGCTCCTATCAGCGGGTCCGCGGGGCGCTTGATACACAGA  360
                                                        M  L  S  S  T  Q  N  A  G  G  S  Y  Q  R  V  R  G  A  L  D  T  Q  K   23
AATGCAGTCCAGAGAAAAGTGCCTCATTTTTCAGTAAAGTGACATATTCCTGGTTTAGCAGAGTAATTACTTTAGGCTATAAGAGACCTTTGGAAAGAGAGGATCTTTTTGAACTAAAGG  480
  C  S  P  E  K  S  A  S  F  F  S  K  V  T  Y  S  W  F  S  R  V  I  T  L  G  Y  K  R  P  L  E  R  E  D  L  F  E  L  K  E   63
AAAGTGATTCCTTCTGCACTGCGTGTCCCATCTTTGAAAAACAATGGAGAAAGGAAGTTTTAAGGAATCAAGAGAGGCAAAAAGTAAAGGTATCTTGTTATAAAGAGGCACATATCAAGA  600
  S  D  S  F  C  T  A  C  P  I  F  E  K  Q  W  R  K  E  V  L  R  N  Q  E  R  Q  K  V  K  V  S  C  Y  K  E  A  H  I  K  K  103
AACCATCTCTACTCTATGCATTGTGGAACACCTTTAAATCCATCCTGATTCAAGTTGCCTTATTCAAAGTGTTTGCTGATATTTTGTCCTTCACTAGCCCACTCATAATGAAGCAAATTA  720
  P  S  L  L  Y  A  L  W  N  T  F  K  S  I  L  I  Q  Y  A  L  F  K  V  F  A  D  I  L  S  F  T  S  P  L  I  M  K  Q  I  I  143
                                                                                    TM1
TCATTTTCTGTGAACACAGCTCAGATTTTGGCTGGAATGGCTATGGCTATGCAGTGGCACTTCTTGTTGTAGTCTTTTTGCAAACTCTGATTCTTCAGCAATATCAACGTTTTAACATGC  840
  I  F  C  E  H  S  S  D  F  G  W  W  G  Y  G  Y  A  V  A  L  L  Y  V  V  F  I  Q  T  L  I  L  Q  Q  Y  Q  R  F  N  M  L  183
                                                                                 TM2
TCACCTCAGCAAAAGTTAAGACAGCTGTAAATGGACTGATCTACAAAAAGGTGTCCCTGGCAACCTTGTGTGTCTATTTCTTACTGGATGAAGGAAACATTTTAACAGCCACTAAAGTGT  960
  T  S  A  K  V  K  I  A  V  N  G  L  I  Y  K  K  V  S  L  A  T  L  C  V  Y  F  L  L  D  E  G  N  I  L  T  A  T  K  V  F  223
                                                      TM3
TCACATCGATGTCTTTGTTTAATATTTTAAGGATTCCTCTGTTTGAGTTACCAACCGTGATCTCAGCTGTGGTCCAGACAAAGATATCCCTGGGCCGTTTGGAAGACTTTCTCAACACTG 1080
  T  S  M  S  L  F  N  I  L  R  I  P  L  F  E  L  P  T  V  I  S  A  V  V  Q  T  K  I  S  L  G  R  L  E  D  F  L  N  T  E  263
                                                TM4
AGGAGCTTCTTCCTCAAAGTATTGAAACGAACTATACAGGAGATCATGCTATTGGGTTTACAGATGCTTCTTTCTCCTCGGATAAAACAGGAATGCCAGTTCTAAAAGAGGCTCTGTGGC 1200
  E  L  L  P  Q  S  I  E  T  N  Y  T  G  D  H  A  I  G  F  T  D  A  S  F  S  W  D  K  T  G  M  P  V  L  K  E  A  L  W  L  303
TTATGTTTCTCAGCAGGCCTGGATTCAGAATTGCATTTTGCAAGAAAACATTCTCTTTGGCTCCATCATGAagaaagagttttatgagcaagtatttggaagcctgtgctctcctttccaga 1320
  M  F  L  S  R  P  G  F  R  I  A  F  C  K  K  T  F  S  L  A  P  S  *                                                    325
tttggagcagttgccaaaggaagatcaaactgaGATTGGAGAAAGAGTAAGGAAACGGCTGTGAATATAAGTGGGGGCCAGCAGCATCGAGTAAGCCTGGCCAGAGCTGTCTACAGTGGG 1440
                                  D  W  R  K  S  K  E  T  A  V  N  I  S  G  G  Q  Q  H  R  V  S  L  A  R  A  V  Y  S  G   29
                                                                                Signature C
GCCGACGTCTACCTCCTGGATGATCCCTTGTCTGCTATTGATGTTCATGTTGGAAAGCAGCTTTTTGAAAAAGTGATAGGGTCCTTGGGCCTTTTGAAAAACCGGGTAGCCATAGTTTCA 1560
A  D  V  Y  L  L  D  D  P  L  S  A  I  D  V  H  V  G  K  Q  L  F  E  K  V  I  G  S  L  G  L  L  K  N  R  V  A  I  Y  S   69
                  Walker B
TTTATGCTTTCTTGTGGGGCAGGGGATATATCTAGCACTGTGCCTAAAATTCCATTTATTTTGTTTATTTGTTGAagcaaagtagtcacatttcacatgaaaaaatgggatgctcagat 1680
F  M  L  S  C  G  A  G  D  I  S  S  T  V  P  K  I  P  F  I  L  F  I  C  *                                             93
tgcaatttcacaggcaaatgtcaatgggtaatttttgaagttttacttacaagtttactctggtgacaatttatgtgattgttatctcttcatctaataccatatcctaagggatgtat 1800
gtgccataatgaattgttgttgactcaagtgatttttacaatggtatttttggtgcacaccaaaatattaataaaattttatattattaacatagcaatttgacattattatcacagcaat 1920
catagtgattcagctgttttgttaaagggccaagaagatgaaaattagtgtttaccagtacatgccatatttcacagggtaaattagttcaatccctatttcacacataaaggagctcag 2040
ggctcacaatgacttgatataggttgctcaacttaagaacaatagagatttttaaaagtatgtctgactccaaagccacattcttcataatatgtgtttatggaattattaatatagaga 2160
actttgaaaatatatgtataaaattataaaatatatgtctcagtaaaaataaacaaacatctttatatattgacataaacccaagattaaaaatgtcacacttaattgtatgtatatgta 2280
taaaataatatgaatgatttaaaaataaggactatgaattatgacttggattaaacactttttttgtaatggtactgtatatttaaaaataagcaagaatgacatatatgaaattgtttt 2400
aaatttgcaattaaattgattcatttctaatgaacgaaaaaatacccgaactaaagtgttaaaaatcacatttagaaactatttttctcatctagcagcatgtcattattccttgtaaaat 2520
acatagatgctgccttaaactggcacctaccaaaaatcatactctgaaatagtaaaggaaaaaagtcattgtagctttttttaaaaagccatttttcgtaatctctgagataaaacactt 2640
tgtttttcagactcatatttttagtgacacacaatctcacacttctgccacaaatgaatcttattgttgtaatgaaaagtggcagaatagctcaaatgggaatataccaggagctgctgtg 2760
taaaaccaaaaatctcactaatttgcaccaagtcatcagtgaacaagaaaaagctcatgctctaaagcaagtcagtgcaatcaactccagaactagaccaaaagacaaaatcctggagca 2880
aaaacatagtgggatatgagtcccctctgagagtcatgcaaggatttctaggcactgttaagaacccacgtagaaagaagatgttaagtgacggtagaaccagttttcagggttgcctg 3000
atttttgaagcagcacttcacagaagtcgaggtgaccaggattgacatgcaagttctaagagacaggccctcattggatcaaggaaaacagctctcaatgaaaaagaaaagatccctg 3120
ttggtgggttgaagttctccatcattctgcagtacctccaagcctttggctggctctgggtgtggctgactgtggtcacttacttagggcagaatttggtgagcattggacagaatctat 3240
ggcttagtgcatgggcaaaagagcaaaaaacatgaatgagttcacagaatggaagcaaataagaagcaataaacttaatatctatggattattgggattaataaaaggtaaaagaaaat 3360
gtaaaaaaaaaaaaaaaaaaaaaaaaa 3389
```

Fig. 1. (A) The genomic structure of *ABCC13* gene on the human chromosome 21. The cytogenetic location of the *ABCC13* gene as well as the structures of exons and introns were analyzed by BLASTN search on the Human Genome Project Working Draft (http://genome.ucsc.edu/). (B) cDNA nucleotide and amino acid sequences of human ABCC13. An in-frame TGA translation stop (over-lined) is present 69 nucleotides upstream of the first methionine codon. The asterisk indicates the translation stop codon. (C) Hydropathy plot of the predicted ABCC13 peptide. Transmembrane domains were predicted using the SOSUI program (http://sosui.proteome.bio.tuat.ac.jp/sosuimenu0.html) and are indicated by TM1–TM4.

21 working draft (GenBank Accession No. AF130358) using the BLASTN program. The *ABCC13* gene is located on human chromosome 21q11.2 and consists of at least 14 exons (Fig. 1A) as predicted from the sequence of the cDNA cloned in this study. Fig. 1B shows the cDNA sequence (3389 bp) of ABCC13 and its deduced amino acid sequences. The longest open reading frame was 978 bp (between +294 and +1271) and had a partial Kozak consensus initiation sequence for translation [31] around the first ATG region, namely, 5′-CGGACC ATG C-3′. This open reading frame encodes a protein consisting of 325 amino acid residues with the starting methionine residue (Fig. 1B). Based on hydropathy and SOSUI analyses, it is suggested that the protein has four transmembrane domains (Figs. 1B and C). Furthermore, protein motif analysis predicted that this peptide has one N-glycosylation site (Asn273) and three protein kinase C phosphorylation sites (Thr21, Thr113, and Ser185).

Fig. 2 shows the partial alignments of the protein with the amino acid sequences of four ABCC trans-

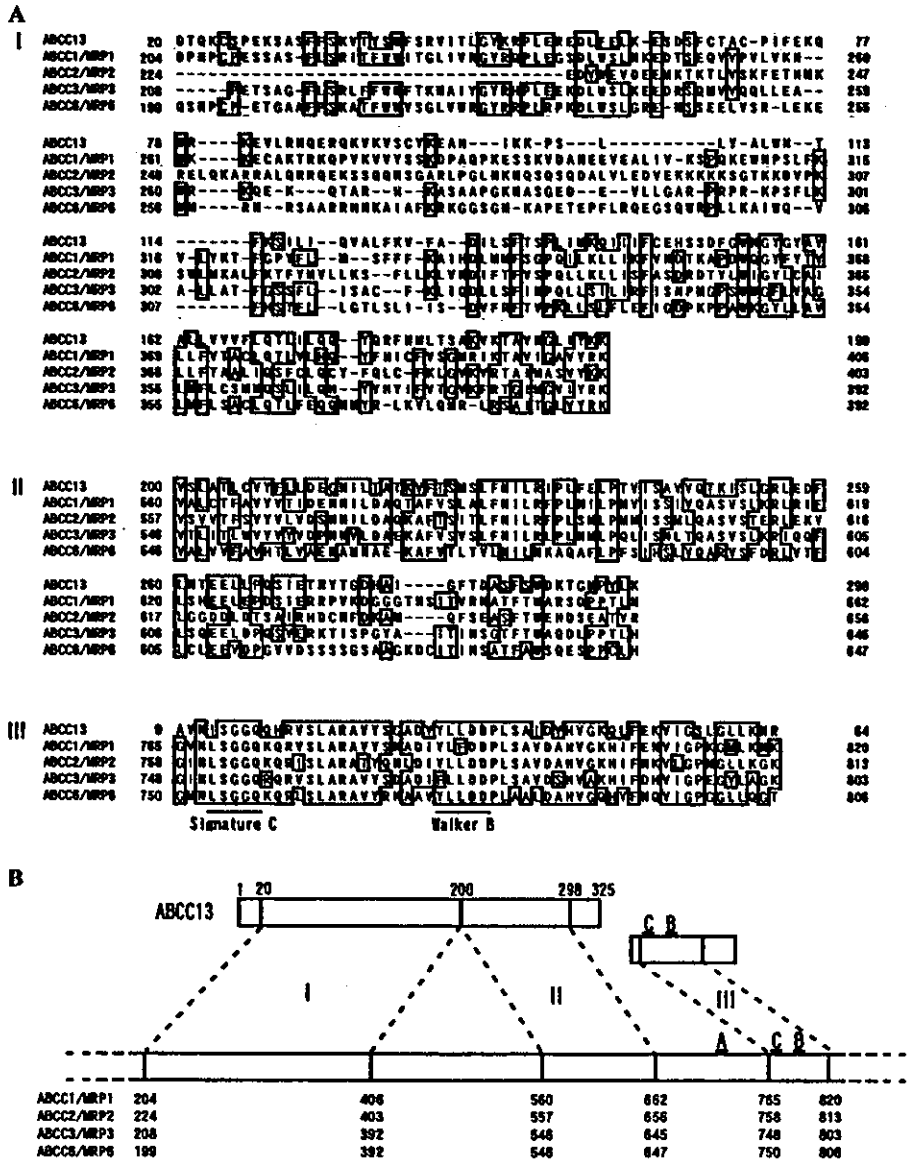

Fig. 2. Multiple alignments of the ABCC13 protein and the putative peptide with ABCC1, ABCC2, ABCC3, and ABCC6. (A) Numbers indicate the positions of amino acid residues. Homology analysis was performed using GENETYX-MAC Version 11 and identical amino acid residues are indicated by boxes. (B) The domains I and II of the ABCC13 protein, as well as the domain III of the putative peptide deduced from the non-coding region (1354–1635) of the ABCC13 cDNA are correlated with those ABC transporters. A, B, and C in the figure indicate Walker A, Walker B, and signature C motifs, respectively. The amino acid sequences of human ABC transporters were acquired from the NCBI database (Accession No. in parentheses): ABCC1/MRP1 (NM004996), human ABCC2/MRP2 (NM000392), human ABCC3/MRP3 (NM003786), and human ABCC6/MRP6 (NM001171).

porters, i.e., ABCC1 (MRP1), ABCC2 (MRP2), ABCC3 (MRP3), and ABCC6 (MRP6). The amino acid sequence form 20 to 298 of the ABCC13 protein is related to those ABC transporters of the sub-family C (domains I and II in Figs. 2A and B). However, the ABCC13 protein lacks Walker A, Walker B, and signature C motifs within the deduced amino acid sequence.

Interestingly, if the region between +1354 and +1635 in the non-coding sequence of the ABCC13 cDNA was translated in a different frame shift, a putative short peptide (93 amino acid residues) could emerge (Fig. 1B). The peptide exhibits remarkably high identities with ABCC1 (MRP1), ABCC2 (MRP2), ABCC3 (MRP3), and ABCC6 (MRP6) and has signature C and Walker B motifs (domain III in Figs. 2A and B). We have searched potential nucleotide sequences corresponding to the Walker A motif throughout the *ABCC13* gene up to the exon 10, however, there is no relevant sequence. In this context, the *ABCC13* gene encodes a non-functional ABC transporter.

Expression profile of human ABCC13

The tissue-specific expression of human ABCC13 was studied by quantitative PCR analysis using human Multiple Tissue cDNA panels (Clontech). As shown in Fig. 3, the mRNA level of ABCC13 was the highest in the fetal liver among the organs studied. Next to the fetal liver, relatively high expression of ABCC13 was detected in the fetal spleen (Fig. 3). It is noteworthy that the expression level of ABCC13 in the fetal liver was approximately 20 times as high as that in the adult liver. Likewise, the expression of ABCC13 in the fetal spleen is 20 times higher than that detected in the adult spleen.

In adult human tissues, colon is the organ where ABCC13 was highly expressed. Lower mRNA levels were observed in several other tissues, including brain, placenta, lung, liver, pancreas, and ovary (adult panel in Fig. 3). In the digestive system, ABCC13 was widely expressed from ileum to rectum, whereas especially highly expression was detected in the colon ascending and transverse (digestive system panel in Fig. 3).

While ABCC13 was expressed in bone marrow cells, its expression in peripheral blood leukocytes of adult humans was several-fold lower. In particular, the expression of ABCC13 was under detection levels in differentiated hematopoietic cells, such as mononuclear cells, resting CD4+ cells, resting CD8+ cells, resting CD14+ cells, resting CD19+ cells, activated mononuclear cells, activated CD4+ cells, activated CD8+ cells, and activated CD19+ cells (blood fraction panel in Fig. 3).

Since the fetal liver expressed ABCC13 at predominantly high levels like the oncofetal α-fetoprotein, we assumed that the expression of this gene might be elevated in cancer. We therefore examined the mRNA levels of ABCC13 in several tumor tissues. Contrary to our expectation, the expression of ABCC13 was not significantly enhanced in lung carcinoma, colon adenocarcinoma, prostate adenocarcinoma, ovarian carci-

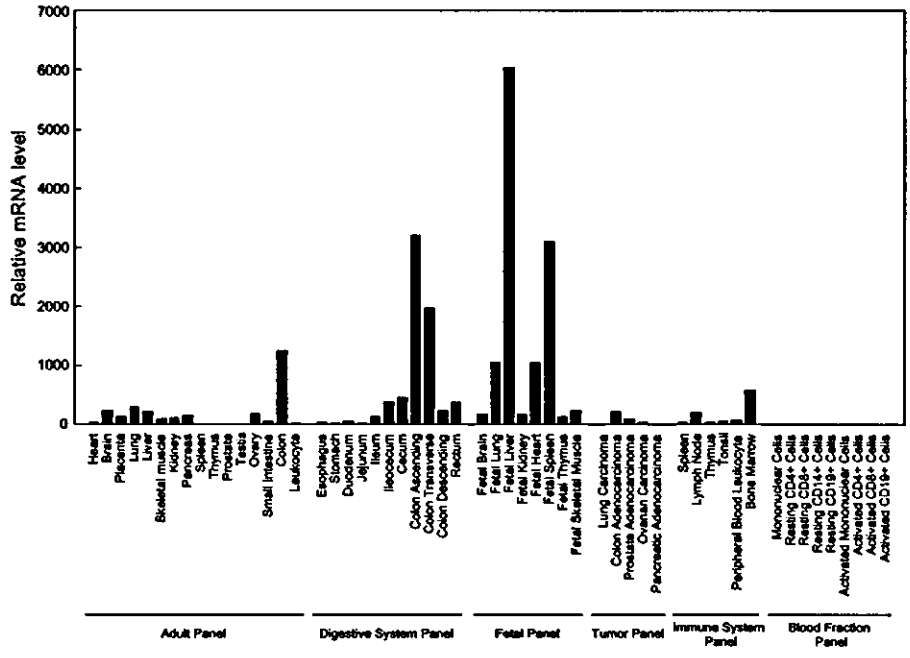

Fig. 3. Relative mRNA levels of ABCC13 detected in different tissues and cell types. Quantitative PCR analysis was carried out in a Smart Cycler system (TaKaRa) using Multiple Tissue cDNA (MTC) Panels, i.e., adult tissues, fetal tissues, digestive system, immune system, tumor, and blood fraction panels (Clontech). The ABCC13-specific primers, i.e., hC13F and hC13B, were used for the PCR (see Materials and methods).

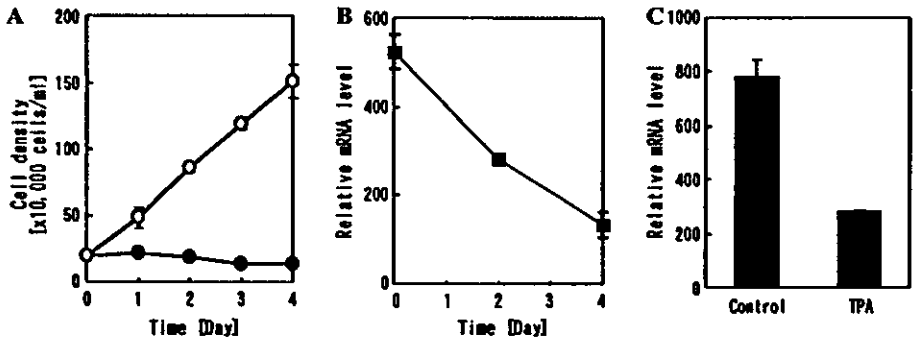

Fig. 4. The effect of TPA on the expression of ABCC13 in K562 cells. (A) Time courses of the growth of K562 cells incubated with (closed circles) and without (open circles) 10 nM TPA. (B) The time course of the ABCC13 mRNA level in K562 cells during incubation with 10 nM TPA. (C) Comparison of relative mRNA levels between TPA-treated and control K562 cells after 2 days of incubation. Results are expressed as means ± SD in triplicate experiments. The levels of ABCC13 mRNA were normalized with β-actin mRNA levels.

noma or pancreatic adenocarcinoma (tumor panel in Fig. 3).

To further examine the expression of ABCC13 in human hepatocarcinoma, we analyzed mRNA levels in tumor and non-tumor regions of biopsy samples by means of quantitative PCR. The mRNA levels of ABCC13 in cancerous regions did not alter, as compared to those in non-cancerous regions in four patients of hepatocellular carcinoma (data not shown). We also examined the expression levels of ABCC13 between tumor regions and non-tumor regions of surgically excised tissue samples from colon carcinoma patients. However, because of wide variations in the expression levels among non-tumor samples, statistically significant results were not obtained.

Expression of ABCC13 in human leukemia K562 cells

Human leukemia K562 cells were found to express ABCC13 at high levels. To study the effect of cell differentiation on the mRNA level of ABCC13, K562 cells were incubated with 10 nM TPA for 4 days. Cell growth was arrested (Fig. 4A) and morphological changes were observed (data not shown). Fig. 4B shows the time course of relative levels of ABCC13 mRNA measured by quantitative PCR. In TPA-treated K562 cells, ABCC13 mRNA level decreased in a time-dependent manner (Fig. 4B), whereas it was maintained almost constant in the control cells during the incubation period. After 2 days, the mRNA level of ABCC13 in TPA-treated K562 cells was approximately one-third of the level in the control cells (Fig. 4C). These results suggest that the expression ABCC13 is down-regulated by cell differentiation in certain leukemia cells.

Concluding remarks

As demonstrated in the present study, the *ABCC13* gene located on chromosome 21q11.2 encodes an unusual truncated peptide that has four transmembrane domains homologous to the ABCC sub-family, but it lacks Walker A, Walker B, and signature C motifs (Figs. 1 and 2). Thus, the *ABCC13* gene encodes a non-functional ABC transporter. Nevertheless, extremely high mRNA levels of ABCC13 in the fetal liver and spleen were noteworthy (Fig. 3). The expression of ABCC13 was detected in bone marrow cells in adult humans. In addition, the mRNA level of ABCC13 in human leukemia K562 cells substantially decreased during cell differentiation (Fig. 4). It has recently been reported that Abcg2, a murine ABC transporter, is expressed at high levels in primitive hematopoietic stem cells and that its expression was sharply down-regulated with cell differentiation [32]. Our preliminary analysis of the promoter region in the 5-kb upstream of the *ABCC13* gene revealed the existence of AML1, GATA-1, and GATA-2 binding motifs (Matsubara and Ishikawa, unpublished work). AML1 is reportedly the target of multiple chromosomal translocations in human leukemia and plays an essential role in fetal liver hematopoiesis [33]. GATA-1 and GATA-2 are critically involved in the development of hematopoietic cells [34–37]. In this context, it is strongly suggested that the expression of the *ABCC13* gene is related with hematopoietic processes in humans.

Acknowledgments

We thank Prof. Masayuki Yamamoto (TARA Center, Tsukuba University, Tsukuba, Japan) for the helpful discussion about the functions of AML1 and GATA and Dr. Shigeki Tarui (GS platZ., Tokyo, Japan) for the generous support to perform this work. Thanks go to Mr. Kiyohiko Matsubara for his help in the promoter analysis. The present study was supported, in part, by research grants entitled "Studies on the genetic polymorphism and function of pharmacokinetics-related proteins in Japanese population" (H12-Genome-026) and "Toxicoproteomics: Expression of ABC transporter genes and drug–drug interactions" (H14-Toxico-002) from the Japanese Ministry of Health and Welfare as well as by a Grant-in-Aid for Creative Scientific Research (No. 13NP0401) and a research Grant (No. 14370754) from the Japan Society for the Promotion of Science.

References

[1] C.F. Higgins, ABC transporters: from microorganisms to man, Annu. Rev. Cell Biol. 8 (1992) 67–113.

[2] I. Klein, B. Sarkadi, A. Varadi, An inventory of the human ABC proteins, Biochim. Biophys. Acta 1461 (1999) 237–262.

[3] M. Dean, A. Rzhetsky, R. Allikmets, The human ATP-binding cassette (ABC) transporter superfamily, Genome Res. 11 (2001) 1156–1166.

[4] P. Borst, R. Evers, M. Kool, J. Wijnholds, The multidrug resistance protein family, Biochim. Biophys. Acta 1461 (1999) 347–357.

[5] T. Ishikawa, Multidrug resistance: genomics of ABC transporters, in: Encyclopedia of Human Genome, Nature Publishing Group, in press (2002).

[6] A. Brooks-Wison, M. Marcil, S.M. Clee, L.-H. Zhang, K. Roomp, M. van Dam, L. Yu, C. Brewer, J.A. Collins, H.O.F. Molhuizen, O. Loubser, B.F.F. Ouelette, K. Fichter, K.J.D. Ashbourne-Excoffon, C.W. Sensen, S. Scherer, S. Mott, M. Denis, D. Martindale, J. Frohlich, K. Morgan, B. Koop, S. Pistone, J.J.P. Kastelein, J. Genest, M.R. Hayden, Mutations in ABC1 in Tangier disease and familial high-density lipoprotein deficiency, Nat. Genet. 22 (1999) 336–345.

[7] M. Bodzioch, E. Orso, J. Klucken, T. Langmann, A. Böttcher, W. Diederich, W. Drobnik, S. Barlage, C. Büchler, M. Porsch-Özcümetz, W.E. Kaminski, H.W. Hahmann, K. Oette, G. Rothe, C. Aslanidis, K.J. Lackner, G. Schmitz, The gene encoding ATP-binding cassette transporter 1 is mutated in Tangier disease, Nat. Genet. 22 (1999) 347–351.

[8] S. Rust, M. Rosier, H. Funke, J. Real, Z. Amoura, J.-C. Piette, J.-F. Deleuze, H.B. Brewer, N. Duverger, P. Denefle, G. Assmann, Tangier disease is caused by mutations in the gene encoding ATP-binding cassette transporter 1, Nat. Genet. 22 (1999) 352–355.

[9] J.R. Riodan, J.M. Rommens, B. Kerem, N. Alon, R. Rozmahel, Z. Grzelczak, J. Zielenski, S. Lokm, N. Plavsic, J.-L. Chou, M.L. Drumm, M.C. Iannuzzi, F.S. Collins, L.-C. Tsui, Identification of the cystic fibrosis gene: cloning and characterization of complementary DNA, Science 245 (1989) 1066–1073.

[10] M. Wada, S. Toh, K. Taniguchi, T. Nakamura, T. Uchiumi, K. Kohno, I. Yoshida, A. Kimura, S. Sakisaka, Y. Adachi, M. Kuwano, Mutations in the canalicular multispecific organic anion transporter (cMOAT) gene, a novel ABC transporter, in patients with hyperbilirubinemia II/Dubin–Johnson syndrome, Hum. Mol. Genet. 7 (1998) 203–207.

[11] R. Allikmets, N.F. Shroyer, N. Singh, J.M. Seddon, R.A. Lewis, P.S. Bernstein, A. Peiffer, N.A. Zabriskie, Y. Li, A. Hutchinson, M. Dean, J.R. Lupski, M. Leppert, Mutation of the Stargardt disease gene (*ABCR*) in age-related macular degeneration, Science 277 (1997) 1805–1807.

[12] K.E. Berge, H. Tian, G.A. Graf, L. Yu, N.V. Grishin, J. Schultz, P. Kwiterovich, B. Shan, R. Barnes, H.H. Hobbs, Accumulation of dietary cholesterol in sitosterolemia caused by mutations in adjacent ABC transporters, Science 290 (2000) 1771–1775.

[13] P. Borst, R. Evers, M. Kool, J. Wijnholds, The multidrug resistance protein family, Biochim. Biophys. Acta 1461 (1999) 347–357.

[14] J. Bryan, L. Aguilar-Bryan, The ABCs of ATP-sensitive potassium channels: more pieces of the puzzle, Curr. Opin. Cell. Biol. 9 (1997) 553–559.

[15] T. Ishikawa, ATP/Mg^{2+}-dependent cardiac transport system for glutathione *S*-conjugates: a study using rat heart sarcolemma vesicles, J. Biol. Chem. 264 (1989) 17343–17348.

[16] T. Ishikawa, Leukotriene C_4 inhibits ATP-dependent transport of glutathione *S*-conjugate across rat heart sarcolemma: implication for leukotriene C_4 translocation mediated by glutathione *S*-conjugate carrier, FEBS Lett. 246 (1989) 177–180.

[17] T. Ishikawa, K. Kobayashi, Y. Sogame, K. Hayashi, Evidence for leukotriene C_4 transport mediated by an ATP-dependent glutathione *S*-conjugate carrier in rat heart and liver plasma membranes, FEBS Lett. 259 (1989) 95–98.

[18] T. Ishikawa, M. Müller, C. Klünemann, T. Schaub, D. Keppler, ATP-dependent primary active transport of cysteinyl leukotrienes across rat liver canalicular membrane: the role of glutathione *S*-conjugate carrier, J. Biol. Chem. 265 (1990) 19279–19286.

[19] T. Ishikawa, The ATP-dependent glutathione *S*-conjugate export pump, Trends Biochem. Sci. 17 (1992) 463–468.

[20] M. Müller, C. Meijer, G.J. Zaman, P. Borst, R.J. Scheper, N.H. Mulder, E.G.E. de Vries, P.L.M. Jansen, Overexpression of the gene encoding the multidrug resistance-associated protein results in increased ATP-dependent glutathione *S*-conjugate transport, Proc. Natl. Acad. Sci. USA 91 (1994) 13033–13037.

[21] G. Jedlitschky, I. Leier, U. Buchholz, K. Barnouin, G. Kurz, D. Keppler, Transport of glutathione, glucuronate, and sulfate conjugates by the MRP gene-encoded conjugate export pump, Cancer Res. 56 (1995) 988–994.

[22] C.C. Paulsuma, P.J. Bosma, G.J. Zaman, C.T. Bakker, M. Otter, G.L. Scheffer, R.J. Scheper, P. Borst, R.P. Oude Elferink, Congential jaundice in rats with a mutation in a multidrug resistance associated protein gene, Science 271 (1996) 1126–1128.

[23] S.P. Cole, G. Bhardwaj, J.H. Gerlach, J.E. Mackie, C.E. Grant, K.C. Almquist, A.J. Stewart, E.U. Kurz, A.M. Duncan, R.G. Deeley, Overexpression of a transporter gene in a multidrug-resistant human lung cancer cell line, Science 258 (1992) 1650–1654.

[24] H. Yabuuchi, H. Shimizu, S. Takayanagi, T. Ishikawa, Multiple splicing variants of two new human ATP-binding cassette transporters, ABCC11 and ABCC12, Biochem. Biophys. Res. Commun. 288 (2001) 933–939.

[25] J. Tammur, C. Prades, I. Arnould, A. Rzhetsky, A. Hutchinson, M. Adachi, J.D. Shuetz, K.J. Swoboda, L.J. Ptacek, M. Rosier, M. Dean, R. Allikmets, Two new genes from the human ATP-binding cassette transporter superfamily, ABCC11 and ABCC12, tandemly duplicated on chromosome 16q12, Gene 273 (2001) 89–96.

[26] T.K. Bera, S. Lee, G. Salvatore, B. Lee, I. Pastan, MRP8, a new member of ABC transporter superfamily, identified by EST database mining and gene prediction program, is highly expressed in breast cancer, Mol. Med. 7 (2001) 509–516.

[27] T.K. Bera, C. Iavarone, V. Kumar, S. Lee, B. Lee, I. Pastan, MRP9, an usual truncated member of the ABC transporter superfamily, is highly expressed in breast cancer, Proc. Natl. Acad. Sci. USA 99 (2002) 6997–7002.

[28] W.-L. Lee, A. Tay, H.-T. Ong, L.-M. Goh, A.P. Monaco, P. Szepetowski, Association of infantile convulsions with paroxysmal dyskinesias (ICCA syndrome): confirmation of linkage to human chromosome 16p12-q12 in a Chinese family, Hum. Genet. 103 (1998) 608–612.

[29] H. Tomita, S. Nagamitsu, K. Wakui, Y. Fukushima, K. Yamada, et al., Paroxysmal kinesigenic choreoathetosis locus maps to chromosome 16p11.2–p12.1, Am. J. Hum. Genet. 65 (1999) 1688–1697.

[30] J. Kyte, R.F. Doolittle, A simple method for displaying the hydropathic character of a protein, J. Mol. Biol. 157 (1982) 105–132.

[31] M. Kozak, An analysis of vertebrate mRNA sequences: intimations of translational control, J. Cell Biol. 115 (1991) 887–903.

[32] S. Zhou, J.D. Schuetz, K.D. Bunting, A.-M. Colapietro, J. Sampath, J.J. Morris, I. Lagutina, G.C. Grosveld, M. Osawa, H. Nakauchi, B.P. Sorrentino, The ABC transporter Bcrp1/ABCG2 is expressed in a wide variety of stem cells and is a molecular

determinant of the side-population phenotype, Nat. Med. 7 (2001) 1028–1034.
[33] T. Okuda, J. van Deursen, S.W. Hiebert, G. Grosveld, J.R. Downing, AML1, the target of multiple chromosomal translocations in human leukemia, is essential for normal fetal liver hematopoiesis, Cell 84 (1996) 321–333.
[34] S.-F. Tsai, D.I.K. Martin, L.I. Zon, A.D. D'Andrea, G.G. Wong, S.H. Orkin, Cloning of cDNA for the major DNA-binding protein of the erythroid lineage through expression in mammalian cells, Nature 339 (1989) 446–451.
[35] S. Takahashi, K. Onodera, H. Motohashi, N. Suwabe, N. Hayashi, N. Yanai, Y. Nabeshima, M. Yamamoto, Arrest in primitive erythroid cell development caused by promoter-specific disruption of the GATA-1 gene, J. Biol. Chem. 272 (1997) 12611–12615.
[36] S. Nishimura, S. Takahashi, T. Kuroha, N. Suwabe, T. Nagasawa, C. Trainor, M. Yamamoto, A GATA box in the *GATA-1* gene hematopoietic enhancer is a critical element in the network of GATA factors and sites that regulate this gene, Mol. Cell. Biol. 20 (2000) 713–723.
[37] F.-Y. Tsai, G. Keller, F.C. Kuo, M. Weiss, J. Chen, M. Rosenblatt, F.W. Alt, S.H. Orkin, An early haematopoietic defect in mice lacking the transcription factor GATA-2, Nature 371 (1994) 221–226.

Jpn. J. Cancer Res. 93, 636–643, June 2002

Identification of Genes Associated with Dedifferentiation of Hepatocellular Carcinoma with Expression Profiling Analysis

Yutaka Midorikawa,[1,3] Shuichi Tsutsumi,[1] Hirokazu Taniguchi,[1] Masami Ishii,[1] Yuko Kobune,[1] Tatsuhiko Kodama,[2] Masatoshi Makuuchi[3] and Hiroyuki Aburatani[1,4]

[1]Genome Science Division and [2]Molecular Biology and Medicine, Research Center for Advanced Science and Technology, University of Tokyo, 4-6-1 Komaba, Meguro-ku, Tokyo 153-8904 and [3]Hepato-Biliary-Pancreatic Surgery Division, Department of Surgery, University of Tokyo, 7-3-1 Hongo, Bunkyo-ku, Tokyo 113-8655

To identify the genes associated with dedifferentiation of hepatocellular carcinoma (HCC), gene expression profiles of HCCs of well-and moderately differentiated grades were compared by means of oligonucleotide arrays. One tumor showed a nodule-in-nodule appearance (NIN), which is occasionally observed in the course of progression of HCC from well to less differentiated grade, when an inner, moderately differentiated tumor (MD) develops sequentially from the outer, well-differentiated tumor (WD). Seventy-six genes were identified to be up-regulated more than 3-fold and 33 genes were down-regulated in the inner nodule in NIN. By statistical analysis of the profiles from 10 individual additional liver tumors, 5 WDs and 5 MDs, we were able to identify 12 genes, *LAMA3*, *PPIB*, *ADAR*, *PSMD4*, *NDUFS8*, *D9SVA*, *CCT3*, *GBAP*, *ARD1*, *RDBP*, *CSRP2*, and *TLE1*, with significantly elevated expression, and 4 genes, *CP*, *IL7R*, *CD48*, and *PLGL*, with decreased expression in MD. These selected genes were further validated using another 12 tumors, 5 WDs and 7 MDs, with semi-quantitative RT-PCR. We also applied neighborhood analysis to list the genes with high predictability values as most closely correlated with WD-MD distinction. Seven genes, *ADAR*, *PSMD4*, *D9SVA*, *CCT3*, *GBAP*, *RDBP*, and *CSRP2*, whose expression was elevated and one gene, *IL7R*, whose expression was decreased, were included among the top 50 predictor genes. These genes are likely to be associated with dedifferentiation of HCC and their identification may help to elucidate the mechanism of liver cancer progression.

Key words: Multistep carcinogenesis — Oligonucleotide array — Nodule-in-nodule appearance — Liver cancer progression — Neighborhood analysis

Recent molecular studies have revealed that development of human cancers is a multistep process.[1)] In hepatocarcinogenesis, early stage hepatocellular carcinoma (HCC), which is small with indistinct margins and consists of well-differentiated cancerous tissues, occasionally gives rise to less differentiated cancerous tissues in the pre-existing well-differentiated tumor during its progression. The internal tumor continues to develop until it finally replaces the nodule.[2)] As such dedifferentiation occurs as a step in multistep hepatocarcinogenesis, nodule-in-nodule appearance can be observed in the course of expansive tumor proliferation.[3)] Thus, a single HCC with nodule-in-nodule appearance (NIN) is best suited to investigate dedifferentiation of HCC, because the inner nodule of lower differentiation grade must have developed sequentially from the well-differentiated outer nodule on the same genetic background.

Thus, multistep hepatocarcinogenesis can be observed in a single tumor macroscopically, although the genetic alterations in each stage are still unknown. In this study, we analyzed the alterations in expression profile of approximately 5600 transcripts in the course of liver cancer progression, using an oligonucleotide array.[4)] Genes which were selected as transcripts with altered expression levels in moderately differentiated hepatocellular carcinoma (MD), when compared to well-differentiated hepatocellular carcinoma (WD) in NIN, were further evaluated by analyzing the expression profiles of 10 independent tumors using oligonucleotide arrays, then validated by analyzing 12 additional tumors by RT-PCR. In addition, we performed neighborhood analysis[5)] to list genes with high predictability values for classification between WD and MD, which included many of the genes we selected above. Our data mining procedure revealed several genes differentially expressed between WD and MD, which have not been reported previously to be associated with dedif-

[4]To whom correspondence should be addressed.
E-mail: haburata-tky@umin.ac.jp

Abbreviations: HCC, hepatocellular carcinoma; WD, well-differentiated hepatocellular carcinoma; MD, moderately differentiated hepatocellular carcinoma; NIN, hepatocellular carcinoma with nodule-in-nodule appearance; RT-PCR, reverse transcription-polymerase chain reaction.

All the gene data are available at the following URL: http://www2.genome.rcast.u-tokyo.ac.jp/database/index.asp

ferentiation of HCC. Their possible involvement in the progression of HCC is discussed.

MATERIALS AND METHODS

Tissue samples Twenty patients with HCC undergoing hepatectomy in Hepato-Biliary-Pancreatic Surgery Division, Department of Surgery, Graduate School of Medicine, University of Tokyo were included in this study after having given their informed consent. Among the 20 hepatectomies, 7 were performed in patients with chronic hepatitis, and the remaining 13 were performed in patients with liver cirrhosis. Twenty-four tumors and corresponding noncancerous liver tissues were obtained from 20 patients, as three patients had multicentric nodules and one patient had NIN. Serologically, 6 patients were hepatitis B surface antigen positive, and 14 patients were hepatitis C virus positive. On the basis of histological findings of the resected specimen, 11 tumors were diagnosed as WD (ON, W1–W10), which is characterized by increased cell density and indefinite nuclear atypia with or without fatty infiltration, and 13 tumors as MD (IN, M1–M12), which is characterized by increased cell density and definite nuclear and structural atypia. One tumor was diagnosed both macroscopically and histologically as NIN, where the differentiation grade was well-differentiated in the outer nodule and moderately differentiated in the inner nodule (Fig. 1). The specimens were immediately cut into small pieces after resection, snap-frozen in liquid nitrogen, and stored at −80°C in a freezer.

RNA extraction and cDNA synthesis Total RNAs were isolated from tissues with "ISOGENE" (Nippon Gene, Tokyo), according to the manufacturer's protocol. Five micrograms of purified total RNA was reverse-transcribed into cDNA, using "SuperScript II" (Life Technologies, Palo Alto, CA) with oligo(dT) primer.

RT-PCR amplification Semi-quantitative RT-PCR amplification with *Taq* polymerase was carried out with a denaturing step at 94°C for 30 s, an annealing step at 63°C for 30 s, and an extension step at 72°C for 60 s. The number of PCR cycles for each gene was optimized so as to distinguish the difference of expression levels between WD and MD, i.e., it should be in the exponential phase before the amplification reaches the plateau level. The primer sequences and number of cycles are listed in Table I. Samples were subjected to electrophoresis on 2% agarose gels and stained with ethidium bromide.

GeneChip protocol Experimental procedures for "GeneChip" were according to the Affymetrix (Santa Clara, CA) GeneChip Expression Analysis Technical Manual, as was described in the previous report.[6] A single expression level for each gene (average difference) was calculated by averaging the differences between matched probes and mismatched probes. Absolute call is judgment of the presence or absence of gene expression, determined by the GeneChip Suite Software.

Identification of genes with expression change in dedifferentiation and statistical analysis We identified the genes whose expression levels were increased during dedifferentiation in three steps. First, in NIN (ON, IN), after we had eliminated all the genes with absolute call as absent in the inner nodule, we selected over-expressed genes whose expression levels were increased more than 3-fold in the inner nodule, compared with the outer nodule, and were not changed between the outer nodule and the non-cancerous liver tissue. Genes that were decreased were also identified: after eliminating the genes with absolute call as absent in the outer nodule, we selected decreased genes whose expression levels were reduced to less than one-third in the inner nodule. Second, the genes thus selected were evaluated by Mann-Whitney U test by comparing the average differences in 10 liver tumors, five WDs (W1–5) and five MDs (M1–5). Differences were considered as significant at $P<0.05$. Third, validation of these genes with altered expression in MD was carried out by semi-quantitative RT-PCR using 12 additional liver tumors, five WDs (W6–10) and seven MDs (M6–12).

Distinction of MD from WD by neighborhood analysis In order to select the predictor genes which distinguish MD from WD, neighborhood analysis was carried out with 6 WDs (ON, W1–5) and 6 MDs (IN, M1–5), as was described in the previous report.[5] Briefly, approximately 5600 genes were sorted by their degree of correlation with the histological groups to list 100 genes (predictor genes) with significant predictive values for classification between WD and MD. For each gene, all expression values among samples were calculated according to the following algorithm as P values.

$$P \text{ value} = (\mu 1 - \mu 2)/(\sigma 1 + \sigma 2),$$

where $\mu 1$ and $\mu 2$ are the average of each group, and $\sigma 1$ and $\sigma 2$ are standard deviation of each group. The P value is the difference between the two means divided by the sum of the standard deviations. According to the P values, the top 50 genes and bottom 50 genes were selected.

RESULTS

To list the genes associated with the dedifferentiation step in liver cancer progression, gene expression profiling analysis was carried out with 12 surgical HCC specimens, that is, the outer and inner nodules in NIN (ON, IN), five WDs (W1–5) and five MDs (M1–5). Semi-quantitative RT-PCR was performed in the outer nodule and inner nodule in NIN (ON, IN) to confirm the results from the second step selection, and five WDs (W6–10) and seven MDs (M6–12) for validation in the third step.

Genes up-regulated in dedifferentiation of HCC

First step: selection of over-expressed genes in NIN (ON, IN) by GeneChip: We selected 2366 genes with absolute call present in the inner nodule in NIN. Among the 2366 genes, we found that expression levels of 94 genes were increased more than 3-fold in the inner nodule, compared with the outer nodule in NIN. Out of these genes, 18 were ruled out because their expression levels in the outer nodule were altered from the non-cancerous tissue, one increased and 17 decreased. Seventy-six genes, therefore, were selected as 'over-expressed genes' in dedifferentiation from WD to MD.

Second step: selection of over-expressed genes using five WDs (W1–5) and five MDs (M1–5) by GeneChip: Using average difference values of the 76 selected genes in the first step, we applied the Mann-Whitney *U* test for statistical analysis, and identified the following 12 genes as significantly increased in a group of WDs, as shown in Fig. 2; *LAMA3* (L34155), laminin, α3; *PPIB* (M63573), peptidylprolyl isomerase B (cyclophilin B); *ADAR* (U10439), adenosine deaminase, RNA specific; *PSMD4* (U24704), proteasome 26S subunit 4; *NDUFS8* (U65579), NADH dehydrogenase Fe-S protein 8; *D9SVA* (U95006), D9 splice variant A; *CCT3* (X74801), chaperonin containing TCP1, subunit 3; *GBAP* (J03060), glucosidase β acid, pseudogene; *ARD1* (X77588), N-acetyltransferase; *RDBP* (L03411), RD RNA-binding protein; *CSRP2* (U46006), cysteine and glycine-rich protein 2; *TLE1* (M99435), transducin-like enhancer of split 1. The GeneChip analysis data for the selected 12 genes were confirmed by semi-quantitative RT-PCR for the two nodules in the NIN tumor. Their expression levels from RT-PCR analysis

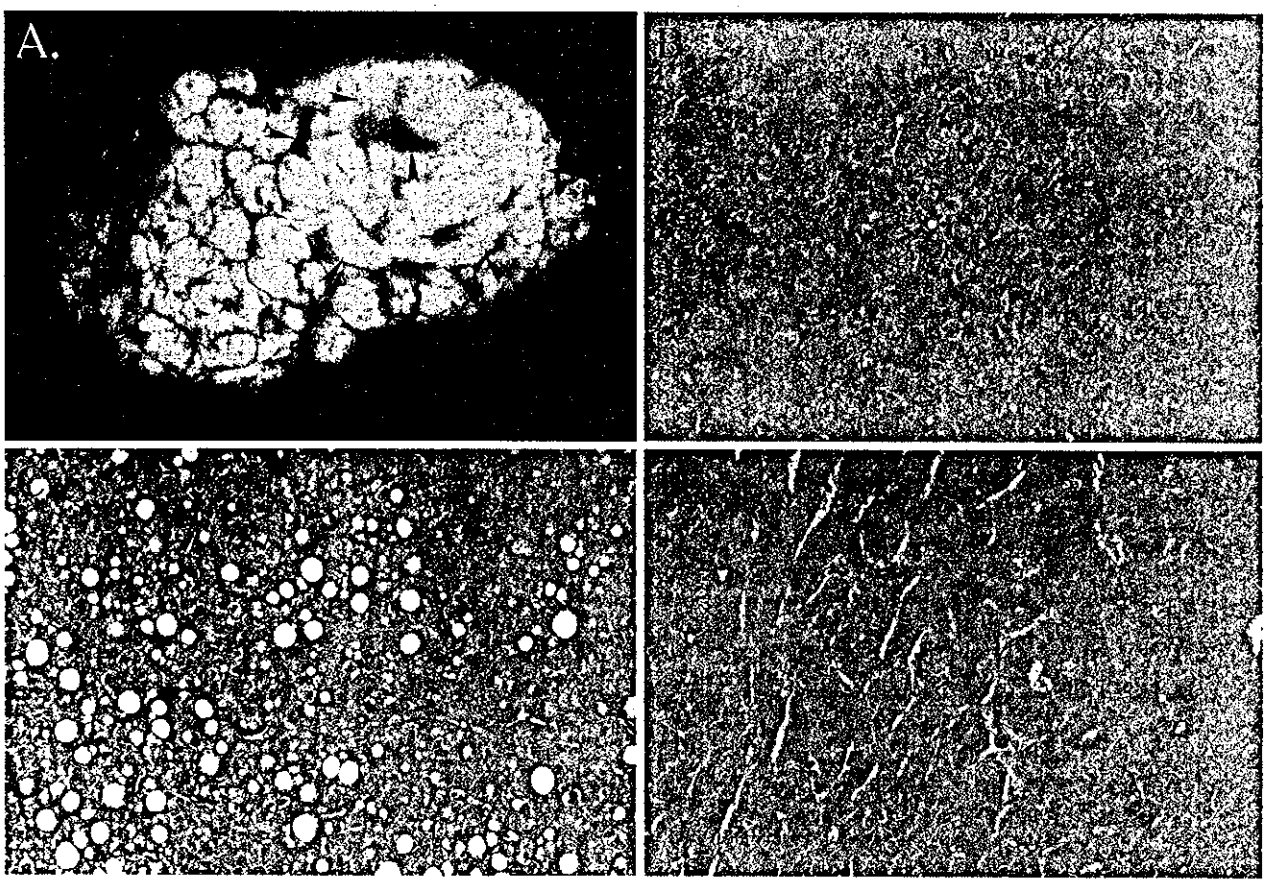

Fig. 1. Pathological findings of the hepatocellular carcinoma with nodule-in-nodule appearance. (A) Macroscopical findings of the tumor. The tumor appeared to be whitish-yellow without capsule formation (arrow), including a green nodule with bile production (arrow). (B) Non-tumor area. (C) Histological findings of the outer nodule, well-differentiated hepatocellular carcinoma. Tumor cells showed resemblance to normal hepatic cells, but decreased cytoplasm, unremarkable nuclear atypia and fatty infiltration. (D) Histological findings of the inner nodule, moderately differentiated hepatocellular carcinoma. Tumor cells showed larger and hyperchromatic nuclei with atypia. The nuclei occupy a relatively greater proportion of the cell.

were apparently concordant with those from GeneChip analysis, although there were relatively subtle differences in *ARD1* and *RDBP* (Fig. 3).

Third step: validation of over-expressed genes using additional WDs (W6–10) and MDs (M6–12) by semi-quantitative RT-PCR: The twelve genes selected above were further examined for validation by semi-quantitative RT-PCR using RNA prepared from 12 additional tumors, five WDs (W6–W10) and seven MDs (M6–M12) (Fig. 3). The intensity of RT-PCR products was higher in a majority of MD cases than in WD cases, which is compatible with the data obtained by GeneChip analysis.

Genes down-regulated in dedifferentiation of HCC Similarly, among 1912 genes with absolute call as present in the outer nodule, 33 were reduced in expression to less than one-third in the inner nodule as compared with the outer nodule of NIN. Among the selected 'decreased genes' in the inner nodule, only four were statistically significantly decreased in expression levels when compared between five WDs (W1–W5) and five MDs (M1–M5), i.e., *CP* (M13699), ceruloplasmin; *IL7R* (M29696), inter-

Table I. Oigonucleotide Pairs Used in RT-PCR Experiments

Gene	Sequence	Cycles
LAMA3	5′-AGGGTGCCATTTCTTCAGCCTC-3′ 5′-GGGTTCTTGGTTTATGCAGTCTCC-3′	35
PPIB	5′-CGCAACATGAAGGTGCTCCTTG-3′ 5′-CGGTCACTCAAAGAAAGATGTCCC-3′	25
ADAR	5′-CCCATCCATTTCAAGGCTATGAG-3′ 5′-CCAGACAGATCATGTGCTGTGG-3′	27
PSMD4	5′-CGGAATGGAGACTTCTTACCCAC-3′ 5′-CCACCTTCACCAGCCAAAATC-3′	23
NDUFS8	5′-GATCCCGAGATGGACATGAAGTC-3′ 5′-CAAGTAGTCAGCCTGGATGTTGG-3′	23
D9SVA	5′-GACAAGACCAAAGAAGCAGCAGTC-3′ 5′-ATCGCATGGCTGGAAAGGTC-3′	25
CCT3	5′-ATTCAAGTCCAGCATCCAGCGG-3′ 5′-AATCCAGCAGCACAATGCGAGG-3′	23
GBAP	5′-CAAGTCCTTCCAGAGAGGAATGTC-3′ 5′-TCAGGGGTGTCTGCATAGGTGTAG-3′	25
ARD1	5′-GGACGAGAATGGGAAGATTGTGG-3′ 5′-TTGACATCTGTGCTCTCTGTGGTC-3′	27
RDBP	5′-TGGTGAAGTCAGGAGCCATCAG-3′ 5′-CGCCGTTCAGGGAATGAATC-3′	25
CSRP2	5′-ACGCAGAAGAGGTGCAGTGTGATG-3′ 5′-ATGAACAAGAGCCCCTGCTCCTTG-3′	25
TLE1	5′-ACAAGAAGCACCACGATGCAG-3′ 5′-TTAACGAGGGGGTCTATGGCTG-3′	30
CP	5′-CCACTGAAGAACAAAGTCCTGGG-3′ 5′-CACTCCTGGACCTGGAAAAAGG-3′	25
IL7R	5′-CACTGACCTGTGCTTTTGAGGAC-3′ 5′-CAAGATGACCAACAGAGCGACAG-3′	30
CD48	5′-GAAGCATGTGCTCCAGAGGTTG-3′ 5′-TGCCATTCTTGCTGCTCACAG-3′	30
PLGL	5′-CAACAACATCCTGGGATTGGGAC-3′ 5′-GCATGGATTTTGGTAGCCACAGG-3′	28

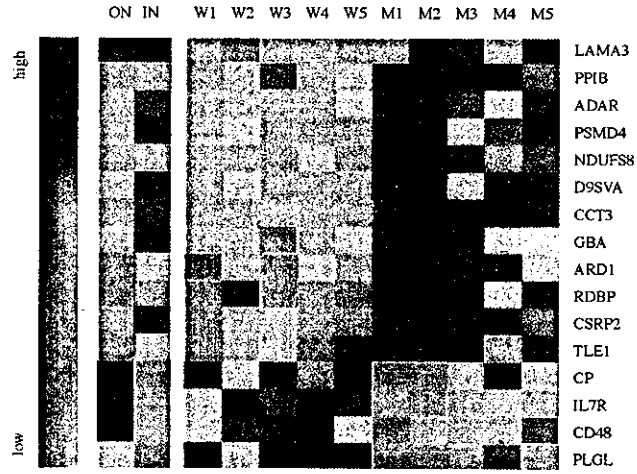

Fig. 2. Genes associated with dedifferentiation of HCC from WD to MD. The 12 genes elevated and the 4 genes decreased in moderately differentiated hepatocellular carcinoma, compared to well-differentiated hepatocellular carcinoma are shown. Each row corresponds to a gene, with the columns corresponding to expression levels in different sample tissues. Expression levels for each gene were normalized across the samples such that the mean is 1 and are shown by relative scales, e.g., expression levels greater than the mean are shown in red, and those below the mean are shown in blue. The scale indicates relative expression above or below the mean. ON, outer nodule in NIN; IN, inner nodule in NIN.

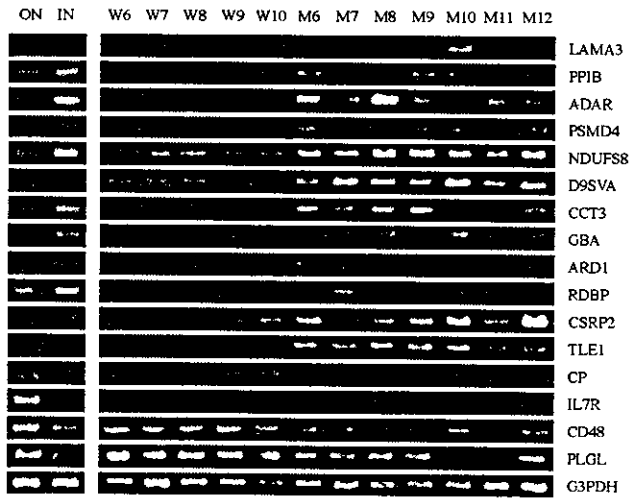

Fig. 3. Semi-quantitative RT-PCR of over-expressed or decreased genes in dedifferentiation from WD to MD. cDNA was synthesized and specific gene segments amplified as indicated in "Materials and Methods." ON, outer nodule in NIN; IN, inner nodule in NIN.

Table II. Top 30 Up-regulated Genes Distinguishing MD from WD

Predictor genes	*P* value
proteasome 26S subunit, ATPase, 5	2.774
cytochrome *c* oxidase subunit VIa polypeptide 1	1.992
chaperonin containing TCP1, subunit 3	**1.983**
prohibitin	1.803
human D9 splice variant B mRNA	**1.753**
proteasome subunit, β, type 4	1.733
hydroxyacyl-coenzyme A dehydrogenase, type II	1.697
peptidylprolyl isomerase A	1.662
adenosine deaminase, RNA-specific	**1.654**
GCN5-like 1	1.591
mitochondrial ribosomal protein L12	1.493
proteasome 26S subunit, non-ATPase, 4	**1.473**
ribosomal protein S10	1.455
cytochrome *c* oxidase subunit VIII	1.452
small nuclear ribonucleoprotein D2 polypeptide	1.435
cysteine and glycine-rich protein 2	**1.331**
laminin receptor 1	1.325
human cell adhesion protein mRNA	1.315
protein kinase C substrate 80K-H	1.312
eukaryotic translation initiation factor 3, subunit 9	1.311
interferon γ receptor 2	1.311
glucosidase, β; acid, pseudogene	**1.291**
proteasome subunit, β type, 3	1.291
transforming growth factor, β3	1.286
H3 histone, family 3A	1.286
ubiquitin A-52 residue ribosomal protein fusion product 1	1.257
neural precursor cell expressed	1.248
RD RNA-binding protein	**1.236**
SMC1-like 1	1.207
uroplakin 1A	1.203

Table III. Top 30 Down-regulated Genes Distinguishing MD from WD

Predictor genes	*P* value
B lymphocyte signal transduction gene	−1.699
Id1 — also represents	−1.524
inositol polyphosphate-5-phosphatase	−1.481
clock (mouse) homolog	−1.403
stromal cell-derived factor 1	−1.373
integrin, αX	−1.339
matrilin 1, cartilage matrix protein	−1.336
zinc finger protein 38	−1.329
fatty-acid-coenzyme A ligase, long-chain 2	−1.324
nuclear factor-like 2	−1.318
complement component 9	−1.306
phosphodiesterase 6B, cGMP-specific, rod, β	−1.276
immunoglobulin κ constant	−1.275
matrix metalloproteinase 15	−1.272
ephrin-B1	−1.263
protein kinase, cAMP-dependent, catalytic, α	−1.26
mitogen-activated protein kinase kinase 3	−1.252
sex hormone-binding globulin	−1.252
H. sapiens mRNA for zinc finger protein	−1.229
caldesmon 1	−1.218
thrombospondin 1	−1.217
small inducible cytokine subfamily A, member 14	−1.207
purinergic receptor P2X, ligand-gated ion channel, 5	−1.201
cyclin I	−1.194
mannose-binding lectin 2, soluble	−1.189
integrin, α1	−1.179
transcription factor 4	−1.167
KIAA0033 protein	−1.165
RAB1, member RAS oncogene family	−1.161
regulator of G-protein signalling 1	−1.157

leukin 7 receptor; *CD48* (M37766), CD48 antigen (B-cell membrane protein); *PLGL* (M93143), plasminogen-like (Fig. 2). Semi-quantitative RT-PCR confirmed the difference in expression of the four genes between the outer and inner nodules in NIN (Fig. 3). Then, these four genes were further validated with semi-quantitative RT-PCR using another set of 12 tumors. The RT-PCR data were well correlated with the GeneChip data (Fig. 3).

Selection of the genes distinguishing WD from MD by neighborhood analysis Using neighborhood analysis on the basis of the expression pattern of about 5600 genes, we found the 100 predictor genes, 50 up-regulated genes and 50 down-regulated genes in MD compared to WD, as being most highly correlated with the WD-MD class distinction. Among these predictor genes, 60 genes including the top 30 genes and the bottom 30 genes are listed in Tables II and III with their *P* values.

In this study, in order to identify the genes regulated during dedifferentiation of HCC, we applied two methods described above, that is, the former method based on progression of HCC and the latter by neighborhood analysis. Seven up-regulated genes, *ADAR*, *PSMD4*, *D9SVA*, *CCT3*, *GBAP*, *RDBP* and *CSRP2*, and one down-regulated gene, *ILR7* were selected in common.

DISCUSSION

A model of multistep tumorigenesis was first proposed by Vogelstein *et al.* in colorectal cancer,[1] i.e., genetic alterations accumulate in each stage of colorectal carcinogenesis, such as polyp, atypical polyp, early-stage cancer and advanced-stage cancer. Hepatocarcinogenesis has also multiple steps to advanced HCC, including adenomatous hyperplasia, WD, MD and poorly differentiated HCC, although the genetic alterations in each stage are not fully

understood.[3] In this study, we performed gene expression profile analysis on WDs and MDs by GeneChip, and to classify liver tumors, we initially applied hierarchical clustering, as described by other investigators.[7-10] However, hierarchical clustering was not very effective to discriminate MDs from WDs in our data (data not shown). Because gene expression profiles are regulated by many factors other than dedifferentiation, unknown conditions not correlated with the WD and MD distinction might have affected the clustering pattern, e.g., lot variation of arrays among the analysis, or hypoxic stress before surgical resection. We, therefore, attempted to identify genes correlated with dedifferentiation by using neighborhood analysis and the analysis of a tumor with NIN in which the inner nodule of NIN must have sequentially developed from the outer nodule. By the latter analysis, we identified 12 genes increased and four genes decreased in MD in comparison to WD, which have not been previously described in the process of dedifferentiation of HCC. These 16 genes were examined by semi-quantitative RT-PCR analysis of 12 additional tumors, five WDs and seven MDs, to validate the selection of genes with altered expression in dedifferentiation of HCC. Furthermore, seven up-regulated genes, *ADAR*, *PSMD4*, *D9SVA*, *CCT3*, *GBAP*, *RDBP* and *CSRP2* and one down-regulated gene, *IL7R*, were listed among the top 50 genes with high predictability value as most closely correlated with WD-MD distinction when used for neighborhood analysis[5] (Tsutsumi, S., unpublished data).

Up-regulation of the nuclear protein TLE1 is intriguing, because TLE1 acts as a co-repressor of AML1, which plays pivotal roles as a transcriptional repressor in myeloid differentiation. TLE1 was also found to influence LEF-1, which is a target of the Wnt signaling pathway by interacting with β-catenin. Another molecule that interacts with TLE1 is hepatic nuclear factor 3b, which is responsible for the basal expression of many liver-specific genes.[11] Further study would be required to understand the transcriptional regulation by TLE1.

RDBP is a component of negative elongation factor (NELF) which is a protein factor required for DRB, a classic inhibitor of transcription elongation by RNA polymerase II, although the function of RDBP is unknown.[12]

The N-terminal of the catalytically active 20S proteasome β-subunits appears to be susceptible to inactivation by N-acetylation. Ard1, together with Nat1, comprises the major N-acetyltransferase in yeast.[13] Up-regulation of ARD1, therefore, might result in inactivation of proteasome activity. PSMD4, a subunit of the 26S protease, binds to ubiquitin polymers and is involved in ubiquitin-dependent and proteasome-mediated protein degradation pathway.[14] Taken together, the results suggest that a protein degradation system acting on a certain substrate is altered in the process of liver cell differentiation.

LAMA3 is α-3 subunit of laminin 5, which, in epithelial basement membranes, forms a complex that functions as a cell adhesion ligand for integrins.[15] CCT3 plays a role in actin and tubulin folding.[16] CSRP2 contains 2 LIM motifs that are implicated in specific protein-protein interactions, particularly involving cytoskeletal components.[17] Presumably, CSRP2 might play a role in liver cell differentiation through interaction with other transcription factors. Altered expression of these genes might be caused through the interaction between liver cancer cells and surrounding cells, then might affect the histological phenotypic patterns of cancer tissues.

PPIB, which enhances the immunosuppressive activity of cyclosporin,[18] plays a role in folding of proteins. Expression levels of PPIB may be increased in accordance with accelerated translation in dedifferentiation of HCC.

ADAR is involved in site-selective RNA editing that changes adenosine residues of target substrate RNAs to inosine.[19] It is critical for embryonic erythropoiesis in the liver, as most ADAR1+/− chimeric embryos died before embryonic day 14 with defects in the hematopoietic system,[20] although its role in hepatocarcinogenesis remains unclear. NDUFS8, coding for the TYKY subunit of the human mitochondrial NADH:ubiquinone oxidoreductase, contains two consensus motifs including four cysteines (CxxCxxCxxxCP) that are presumed to ligand two [4Fe-4S] iron-sulfur clusters. This feature makes the TYKY subunit a prominent subunit directly involved in the electron transfer process.[21] The mechanism of the altered expression of GBAP[22] and D9SVA is unknown.

As for down-regulated genes, expression of CP might be decreased in the course of dedifferentiation, as CP is produced in normal hepatocytes.[23] Cancer-mediated proteolysis of plasminogen generates angiostatin, which is a potent endogenous inhibitor of angiogenesis.[24] PLGL, which has a homologous sequence to plasminogen, showed down-regulation. On the other hand, the association of liver cell dedifferentiation and decreased expression of IL-7 and CD48, B-cell membrane protein, remains unclear.[25,26] The present study analyzed the bulk cancerous tissues, which contain many different cell types other than liver cancer cells. Further experiments, such as expression profiling using microdissected tissues, would provide more accurate information about which cell types express those transcripts.

In summary, this study has identified genes with altered expression in dedifferentiation from WD to MD, by means of gene expression profiling analysis. By applying two different data mining methods, we identified genes that showed significantly altered expression, 12 increased and four decreased, in association with dedifferentiation from WD to MD. Further evaluation of those genes would be required to elucidate their possible involvement in dedifferentiation of HCC.

ACKNOWLEDGMENTS

We thank Yoshitaka Hippo and Sarah Kim for critical reading of the manuscript, and Hiroko Meguro and Erio Ashihara for valuable technical assistance. This work was supported in part by Grants-in-Aid for Scientific Research (B) 09557014 and 10470131 and Scientific Research on Priority Areas (C) 12217031 from the Ministry of Education, Culture, Sports, Science and Technology (H. A.)

(Received February 18, 2002/Revised April 2, 2002/Accepted April 5, 2002)

REFERENCES

1) Vogelstein, B., Fearon, E. R., Hamilton, S. R., Kern, S. E., Preisinger, A. C., Leppert, M., Nakamura, Y., White, R., Smits, A. M. and Bos, J. L. Genetic alterations during colorectal-tumor development. *N. Engl. J. Med.*, **319**, 525–532 (1988).
2) Kojiro, M. Pathology of early hepatocellular carcinoma: progression from early to advanced. *Hepatogastroenterology*, **45** (Suppl. 3), 1203–1205 (1998).
3) Nakashima, O., Sugihara, S., Kage, M. and Kojiro, M. Pathomorphologic characteristics of small hepatocellular carcinoma: a special reference to small hepatocellular carcinoma with indistinct margins. *Hepatology*, **22**, 101–105 (1995).
4) Lockhart, D. J., Dong, H., Byrne, M. C., Follettie, M. T., Gallo, M. V., Chee, M. S., Mittmann, M., Wang, C., Kobayashi, M., Horton, H. and Brown, E. L. Expression monitoring by hybridization to high-density oligonucleotide arrays. *Nat. Biotechnol.*, **14**, 1675–1680 (1996).
5) Golub, T. R., Slonim, D. K., Tamayo, P., Huard, C., Gaasenbeek, M., Mesirov, J. P., Coller, H., Loh, M. L., Downing, J. R., Caligiuri, M. A., Bloomfield, C. D. and Lander, E. S. Molecular classification of cancer: class discovery and class prediction by gene expression monitoring. *Science*, **286**, 531–537 (1999).
6) Ishii, M., Hashimoto, S., Tsutsumi, S., Wada, Y., Matsushima, K., Kodama, T. and Aburatani, H. Direct comparison of GeneChip and SAGE on the quantitative accuracy in transcript profiling analysis. *Genomics*, **68**, 136–143 (2000).
7) Xu, X. R., Huang, J., Xu, Z. G., Qian, B. Z., Zhu, Z. D., Yan, Q., Cai, T., Zhang, X., Xiao, H. S., Qu, J., Liu, F., Huang, Q. H., Cheng, Z. H., Li, N. G., Du, J. J., Hu, W., Shen, K. T., Lu, G., Fu, G., Zhong, M., Xu, S. H., Gu, W. Y., Huang, W., Zhao, X. T., Hu, G. X., Gu, J. R., Chen, Z. and Han, Z. G. Insight into hepatocellular carcinogenesis at transcriptome level by comparing gene expression profiles of hepatocellular carcinoma with those of corresponding noncancerous liver. *Proc. Natl. Acad. Sci. USA*, **98**, 15089–15094 (2001).
8) Okabe, H., Satoh, S., Kato, T., Kitahara, O., Yanagawa, R., Yamaoka, Y., Tsunoda, T., Furukawa, Y. and Nakamura, Y. Genome-wide analysis of gene expression in human hepatocellular carcinomas using cDNA microarray: identification of genes involved in viral carcinogenesis and tumor progression. *Cancer Res.*, **61**, 2129–2137 (2001).
9) Shirota, Y., Kaneko, S., Honda, M., Kawai, H. F. and Kobayashi, K. Identification of differentially expressed genes in hepatocellular carcinoma with cDNA microarrays. *Hepatology*, **33**, 832–840 (2001).
10) Lau, W. Y., Lai, P. B., Leung, M. F., Leung, B. C., Wong, N., Chen, G., Leung, T. W. and Liew, C. T. Differential gene expression of hepatocellular carcinoma using cDNA microarray analysis. *Oncol. Res.*, **12**, 59–69 (2000).
11) Wang, J. C., Waltner-Law, M., Yamada, K., Osawa, H., Stifani, S. and Granner, D. K. Transducin-like enhancer of split proteins, the human homologs of *Drosophila* groucho, interact with hepatic nuclear factor 3beta. *J. Biol. Chem.*, **275**, 18418–18423 (2000).
12) Yamaguchi, Y., Takagi, T., Wada, T., Yano, K., Furuya, A., Sugimoto, S., Hasegawa, J. and Handa, H. NELF, a multisubunit complex containing RD, cooperates with DSIF to repress RNA polymerase II elongation. *Cell*, **97**, 41–51 (1999).
13) Arendt, C. S. and Hochstrasser, M. Eukaryotic 20S proteasome catalytic subunit propeptides prevent active site inactivation by N-terminal acetylation and promote particle assembly. *EMBO J.*, **18**, 3575–3585 (1999).
14) Deveraux, Q., Ustrell, V., Pickart, C. and Rechsteiner, M. A 26S protease subunit that binds ubiquitin conjugates. *J. Biol. Chem.*, **269**, 7059–7061 (1994).
15) Torimura, T., Ueno, T., Kin, M., Ogata, R., Inuzuka, S., Sugawara, H., Kurotatsu, R., Shimada, M., Yano, H., Kojiro, M., Tanikawa, K. and Sata, M. Integrin alpha6beta1 plays a significant role in the attachment of hepatoma cells to laminin. *J. Hepatol.*, **31**, 734–740 (1999).
16) Frydman, J., Nimmesgern, E., Erdjument-Bromage, H., Wall, J. S., Tempst, P. and Hartl, F. U. Function in protein folding of TRiC, a cytosolic ring complex containing TCP-1 and structurally related subunits. *EMBO J.*, **11**, 4767–4778 (1992).
17) Konrat, R., Krautler, B., Weiskirchen, R. and Bister, K. Structure of cysteine- and glycine-rich protein CRP2. Backbone dynamics reveal motional freedom and independent spatial orientation of the lim domains. *J. Biol. Chem.*, **273**, 23233–23240 (1998).
18) Denys, A., Allain, F., Masy, E., Dessain, J. P. and Spik, G. Enhancing the effect of secreted cyclophilin B on immunosuppressive activity of cyclosporine. *Transplantation*, **65**, 1076–1084 (1998).
19) Maas, S., Gerber, A. P. and Rich, A. Identification and characterization of a human tRNA-specific adenosine deaminase related to the ADAR family of pre-mRNA editing enzymes. *Proc. Natl. Acad. Sci. USA*, **96**, 8895–8900

(1999).
20) Wang, Q., Khillan, J., Gadue, P. and Nishikura, K. Requirement of the RNA editing deaminase ADAR1 gene for embryonic erythropoiesis. *Science*, **290**, 1765–1768 (2000).
21) de Sury, R., Martinez, P., Procaccio, V., Lunardi, J. and Issartel, J. P. Genomic structure of the human NDUFS8 gene coding for the iron-sulfur TYKY subunit of the mitochondrial NADH:ubiquinone oxidoreductase. *Gene*, **215**, 1–10 (1998).
22) Horowitz, M., Wilder, S., Horowitz, Z., Reiner, O., Gelbart, T. and Beutler, E. The human glucocerebrosidase gene and pseudogene: structure and evolution. *Genomics*, **4**, 87–96 (1989).
23) Casaril, M., Capra, F., Marchiori, L., Gabrielli, G. B., Nicoli, N., Corso, F., Baracchino, F. and Corrocher, R. Serum copper and ceruloplasmin in early and in advanced hepatocellular carcinoma: diagnostic and prognostic relevance. *Tumori*, **75**, 498–502 (1989).
24) Cao, R., Wu, H. L., Veitonmaki, N., Linden, P., Farnebo, J., Shi, G. Y. and Cao, Y. Suppression of angiogenesis and tumor growth by the inhibitor K1-5 generated by plasmin-mediated proteolysis. *Proc. Natl. Acad. Sci. USA*, **96**, 5728–5733 (1999).
25) Trinder, P., Seitzer, U., Gerdes, J., Seliger, B. and Maeurer, M. Constitutive and IFN-gamma regulated expression of IL-7 and IL-15 in human renal cell cancer. *Int. J. Oncol.*, **14**, 23–31 (1999).
26) Li, Y., Hellstrom, K. E., Newby, S. A. and Chen, L. Costimulation by CD48 and B7-1 induces immunity against poorly immunogenic tumors. *J. Exp. Med.*, **183**, 639–644 (1996).

[CANCER RESEARCH 62, 233–240, January 1, 2002]

Global Gene Expression Analysis of Gastric Cancer by Oligonucleotide Microarrays[1]

Yoshitaka Hippo, Hirokazu Taniguchi, Shuichi Tsutsumi, Naoko Machida, Ja-Mun Chong, Masashi Fukayama, Tatsuhiko Kodama, and Hiroyuki Aburatani[2]

Genome Science Division [Y. H., H. T., S. T., N. M., H. A.] and Division of Molecular Biology and Medicine [T. K.], Research Center for Advanced Science and Technology and Department of Pathology, Graduate School of Medicine [H. T., J-M. C., M. F.], The University of Tokyo, Tokyo 153-8904, Japan

ABSTRACT

To gain molecular understanding of carcinogenesis, progression, and diversity of gastric cancer, 22 primary human advanced gastric cancer tissues and 8 noncancerous gastric tissues were analyzed by high-density oligonucleotide microarray in this study. Based on expression analysis of approximately 6800 genes, a two-way clustering algorithm successfully distinguished cancer tissues from noncancerous tissues. Subsequently, genes that were differentially expressed in cancer and noncancerous tissues were identified; 162 and 129 genes were highly expressed ($P < 0.05$) >2.5-fold in cancer tissues and noncancerous tissues, respectively. In cancer tissues, genes related to cell cycle, growth factor, cell motility, cell adhesion, and matrix remodeling were highly expressed. In noncancerous tissues, genes related to gastrointestinal-specific function and immune response were highly expressed. Furthermore, we identified several genes associated with lymph node metastasis including *Oct-2* or histological types including *Liver-Intestine Cadherin*. These results provide not only a new molecular basis for understanding biological properties of gastric cancer, but also useful resources for future development of therapeutic targets and diagnostic markers for gastric cancer.

INTRODUCTION

Gastric cancer is one of the leading causes of cancer death in the world (1). Advances in diagnostic and treatment technologies have enabled us to offer excellent long-term survival results for early gastric cancer, but prognosis of advanced gastric cancer still remains poor (2). Recent molecular analyses have clarified many genetic alterations in gastric carcinogenesis, such as *p53* (3), *β-catenin* (4), *E-cadherin* (5), *trefoil factor 1* (6), and *c-met* (7), but this is hardly sufficient to understand common pathway of carcinogenesis and progression of gastric cancer. Furthermore, gastric cancer shows diverse clinical properties such as histological type, metastatic status, invasiveness, and responsiveness to chemotherapy. Little is known about the genes associated with these characteristics.

Gastric cancer tissues generally contain multiple nonepithelial cell types such as fibroblast, smooth muscle cell, endothelial cell, infiltrating lymphocyte, and macrophage. Because recent advances in cancer research have revealed the relevance of epithelial-stromal interaction including ECMs,[3] MMPs, and angiogenic factors in cancer progression (8, 9), we have analyzed whole cancer tissues in this study instead of focusing only on cancer cells to better describe the entire aspect of gastric cancer.

Array technologies are accurate and comprehensive ways of simultaneously analyzing the expression of thousands of genes and have been rapidly applied in many research fields (10). To clarify gene expression changes that are common in cancer tissues or differ among cancer tissues, we have analyzed gastric cancer by oligonucleotide microarray representing approximately 5600 unique genes in this study. We classified both samples and genes by a two-way clustering analysis and identified genes that were differentially expressed between cancer and noncancerous tissues. Furthermore, several genes were identified as being associated with lymph node metastasis or histological types by comparing array data with clinicopathological data.

MATERIALS AND METHODS

Tissue Samples and RNA Preparation. Twenty-six pairs of advanced gastric cancer tissues (T1–T26) and corresponding adjacent noncancerous gastric tissues (N1–N26) were obtained with informed consent from patients who underwent gastrectomy at Jichi Medical College Hospital (Tochigi, Japan). Depth of invasion was more than muscularis propria for all of the cancer tissues, some of which were diagnosed microscopically to accompany lymph node metastasis. A pathologist (J-M. C.) dissected tissue samples from surgical specimens with special care for minimal contamination of nonepithelial cells, and samples were immediately snap-frozen in liquid nitrogen. Another pathologist (H. T.) determined histological classification according to Lauren's classification (11) after H&E staining. These clinical and histopathological features are summarized in Table 1.Tissues were homogenized and lysed directly in Isogen reagent (Nippon Gene, Osaka, Japan). Total RNA was extracted according to the manufacturer's instructions only from tumor specimens that contained >50% cancer cells.

High-density Oligonucleotide Microarray Analysis. Twenty-two gastric cancers (T1–T22) and 8 noncancerous gastric tissues (3N, 4N, 9N, 12N, 16N, and 22N–24N) were analyzed by oligonucleotide microarray (GeneChip HuGeneFL array; Affymetrix, Santa Clara, CA). This array contains 6936 probes interrogating approximately 5600 full-length human genes from the Unigene (Build 18), GenBank, and The Institute for Genomic Research. Analysis was performed essentially as described previously (12). Briefly, double-stranded cDNA was synthesized from 10 μg of total RNA with oligo$(dT)_{24}$ T7 primer, amplified with T7 RNA polymerase up to approximately 100 μg of cRNA, and hybridized to the oligonucleotide microarray according to manufacturer's instructions. For normalization, the average intensity for 6936 genes in total was made equal to 100 to reliably compare variable multiple arrays.

Statistical Analysis. A two-way clustering analysis of 30 samples by Pearson's correlation was performed using the 6272 genes that passed prefiltering, which eliminated genes with an expression level <10 for all of the samples. To identify genes that were differentially expressed between the two groups, Mann-Whitney's U test was used with significance set at $P < 0.05$. Genespring (Silicon Genetics, Redwood City, CA) was used for clustering and statistical analysis. The average expression level of each gene in each group (Ca, cancer tissue; N, noncancerous tissue) was calculated, value below 10 was set to 10, and then the ratio of average expression level between the two groups (Ca:N or N:Ca) was calculated. The cutoff value was set to 80 for average expression level and to 2.5 or 2.0 for the ratio.

Semiquantitative RT-PCR. Single-stranded cDNA was synthesized with oligo(dT) primer in a 20-μl reaction from 5 μg of total RNA using SuperScript

Received 7/31/01; accepted 11/7/01.

The costs of publication of this article were defrayed in part by the payment of page charges. This article must therefore be hereby marked *advertisement* in accordance with 18 U.S.C. Section 1734 solely to indicate this fact.

[1] Supported in part by Grants-in-Aid for Scientific Research (B) 10470131 and 13470114 from the Ministry of Education, Culture, Sports, Science and Technology, and by funds from Uehara Memorial Foundation (to H. A.). This study was carried out as a part of The Technology Development for Analysis of Protein Expression and Interaction in Bioconsortia on R&D of New Industrial Science and Technology Frontiers that was performed by Industrial Science, Technology and Environmental Policy Bureau, Ministry of Economy, Trade & Industry and delegated to New Energy Development Organization.

[2] To whom requests for reprints should be addressed, at Genome Science Division, Research Center for Advanced Science and Technology, The University of Tokyo, 4-6-1 Komaba, Meguro-ku, Tokyo 153-8904, Japan. Phone: 81-3-5452-5235; Fax: 81-3-5452-5355; E-mail: haburata-tky@umin.ac.jp.

[3] The abbreviations used are: ECM, extracellular matrix; MMP, matrix metalloproteinase; RT-PCR, reverse transcription-PCR; LI-cadherin, liver intestine cadherin.

Table 1 *Histopathological characterization of cancer tissue samples*

Histological classification, lymph node metastasis status, and immunoreactivity to anti-p53, E-cadherin, and β-catenin antibodies are described (++, positive for >50%; +, positive for <50%; −, negative). Nuclear staining is regarded positive for p53 and β-catenin, whereas membranous staining is regarded positive for E-cadherin.

Sample	Patient	Histology	Metastasis	p53	E-cadherin	β-Catenin
T1	J-159	Diffuse	−	−	−	+
T2	J-258	Diffuse	+	++	−	−
T3	J-290	Diffuse	+	−	+	−
T4	J-133	Diffuse	+	++	+	−
T5	J-108	Diffuse	+	−	−	+
T6	J-111	Intestinal	+	++	+	++
T7	J-199	Intestinal	+	−	+	−
T8	J-125	Intestinal	+	++	+	++
T9	J-128	Intestinal	−	+	+	+
T10	J-163	Intestinal	+	+	+	−
T11	J-175	Intestinal	+	+	+	−
T12	J-191	Intestinal	−	++	+	−
T13	J-194	Intestinal	+	−	+	−
T14	J-256	Intestinal	−	++	+	−
T15	J-264	Intestinal	−	+	+	++
T16	J-277	Intestinal	−	++	+	++
T17	J-166	Intestinal	+	−	+	+
T18	J-209	Intestinal	−	+	+	+
T19	J-222	Intestinal	+	−	+	−
T20	J-274	Intestinal	+	−	+	−
T21	J-275	Intestinal	+	++	+	−
T22	J-287	Intestinal	+	++	+	−

Preamplification System for First Strand cDNA Synthesis System (Life Technologies, Inc., Rockville, MD) and diluted up to 80 μl. PCR was then performed with 1 μl of cDNA for 1 cycle of 94°C for 2 min, followed by 20–30 cycles of 94°C for 30 s, 60°C for 30 s, and 72°C for 3 min using gene-specific primers and Taq polymerase. Amplification of the right target DNA was confirmed by mobility on gel electrophoresis and sequencing after subcloning into pGEM-T easy vector (Promega, Madison, WI). β-Actin was used as an internal control to confirm equal amount of the templates.

Immunohistochemistry. Formalin-fixed, paraffin-embedded gastric cancer sections were immunostained with horseradish peroxidase-conjugated secondary antibodies using the DAKO LSAB2/HRP kit (DAKO JAPAN, Kyoto, Japan) following the manufacturer's instructions. Primary antihuman antibodies were diluted 1:100 for p53 (DO-7; Novocastra Laboratories Ltd., Newcastle, United Kingdom), 1:1000 for β-catenin (BD; Transduction Laboratories, Lexington, KY), 1:500 for E-cadherin (HECD-1; Takara, Tokyo, Japan), and 1:500 for Oct-2 (C-20; Santa Cruz Biotechnology, Inc., Santa Cruz, CA).

RESULTS

A Two-way Clustering Analysis of Gastric Cancer and Noncancerous Tissues. Twenty-two advanced gastric cancer tissues and 8 noncancerous tissues were analyzed by oligonucleotide microarray, and expression data for 6936 genes were obtained. With expression data of 6272 expressed genes that passed prefiltering, a two-way clustering analysis according to Pearson's correlation was performed. Cancer tissues and noncancerous tissues (30 samples in total) were successfully distinguished (Fig. 1). However, this algorithm using most of the genes on the array did not classify samples among cancer tissues by subgroups associated with histopathological features such as those listed in Table 1.

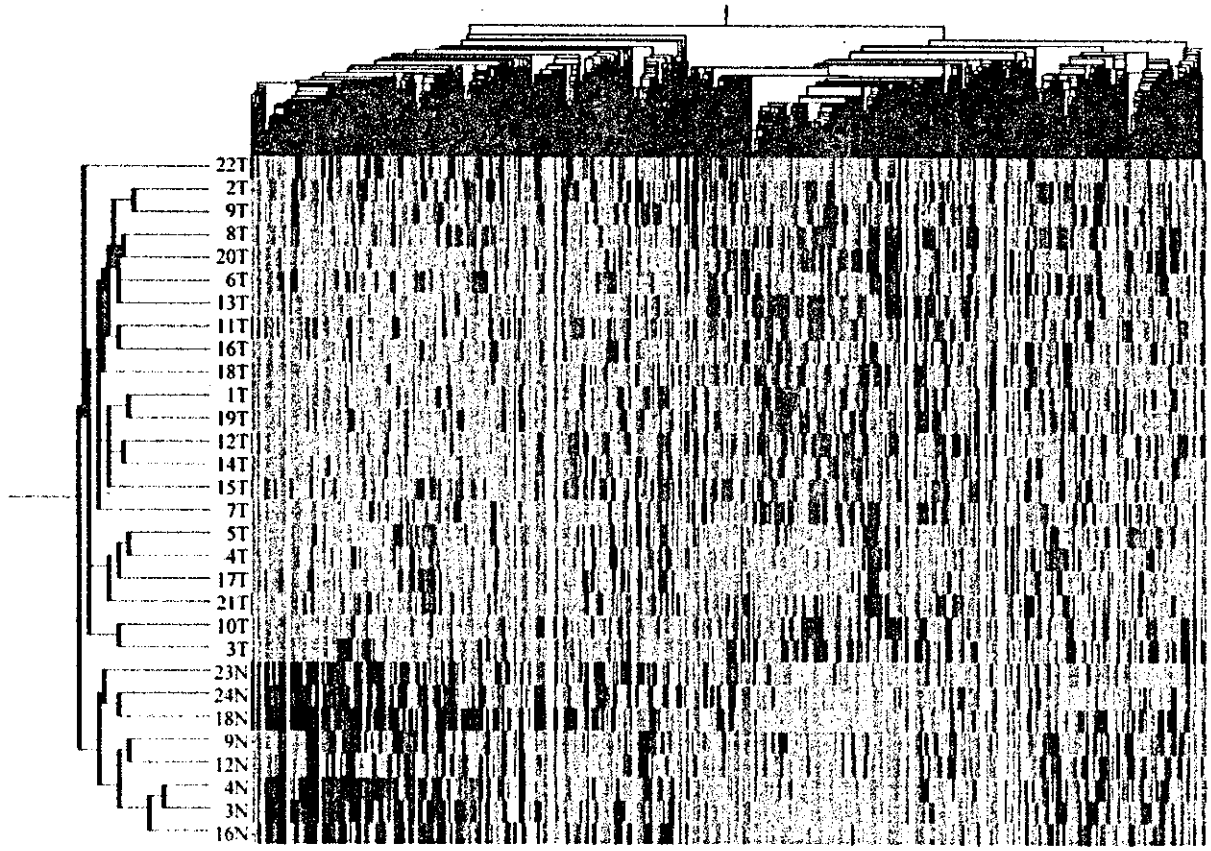

Fig. 1. A two-way clustering analysis of gastric cancer and noncancerous tissues. Thirty samples are lined up on the *vertical axis*, and 6272 genes are in the *horizontal axis*. Cancer tissues (*T*) and noncancerous tissues (*N*) were distinguished. Expression level was normalized per gene, and the relative value to the median among 30 samples is shown by color: *red*; relatively high expression, *blue*; relatively low expression.

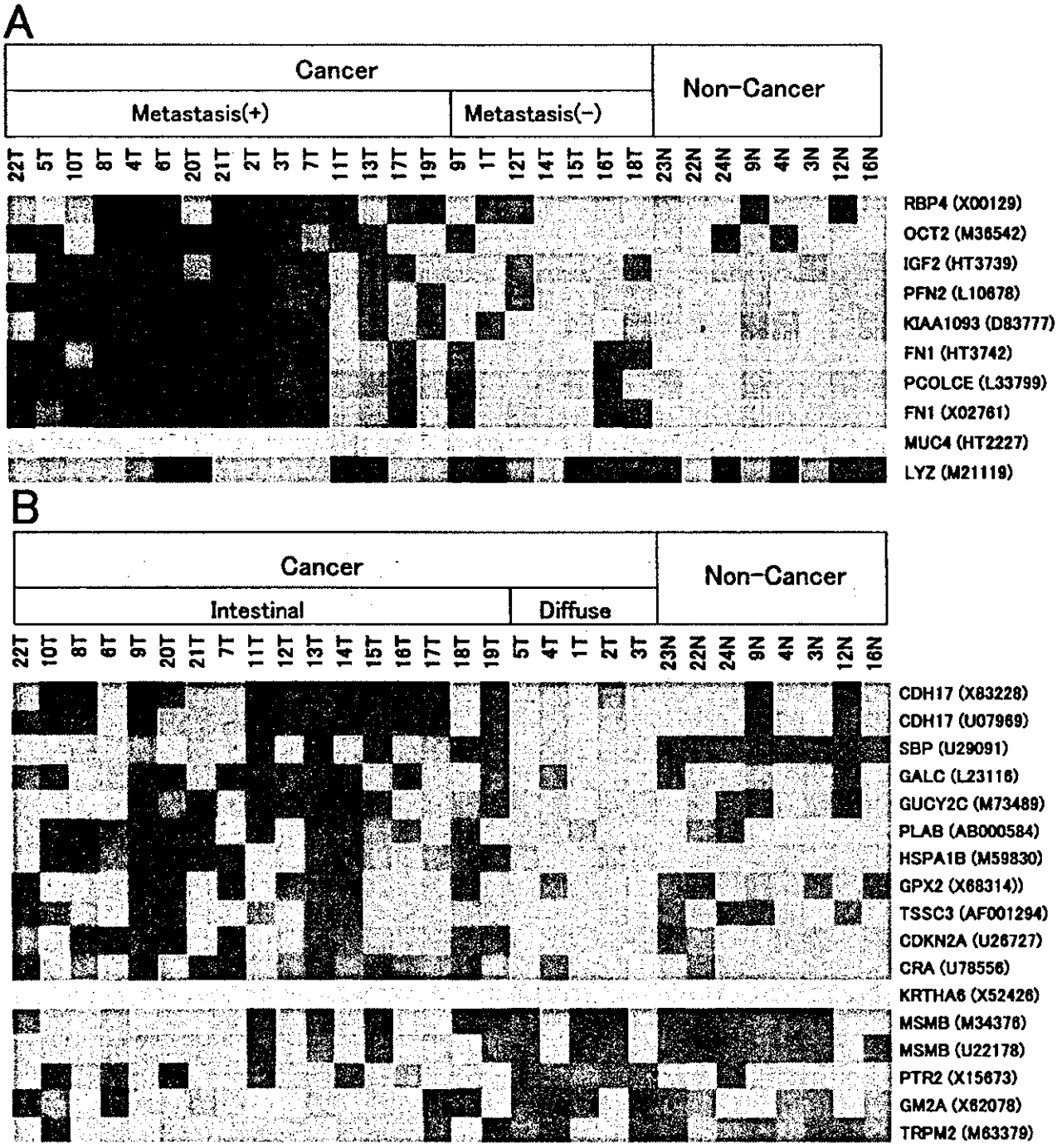

Fig. 2. Genes associated with clinicopathological properties of gastric cancer. Expression level was normalized per gene, and the relative value to the median among 30 samples is shown by color: *red*; relatively high expression, *blue*; relatively low expression. Cutoff value was set to 80 for average intensity and to 2.0 for ratio. GenBank accession numbers are given in *parentheses*. *A*, genes associated with lymph node metastasis. Genes with exclusively high or low expression in metastasis-positive cancer tissues are shown. *B*, genes associated with histological classification. Genes differentially expressed between intestinal-type and diffuse-type cancer are shown. Noncancerous tissue samples are also shown, but only for reference.

Highly Expressed Genes in Gastric Cancer and Noncancerous Tissues. To identify genes that were differentially expressed between cancer and noncancerous tissues, we applied Mann-Whitney's U test to the raw data obtained by microarray analysis. When cutoff values were set to 2.5 for the ratio and 80 for the average expression level to extract only reliable data, 162 and 129 genes were identified that showed higher expression in cancer tissues and noncancerous tissues, respectively ($P < 0.05$). To verify the reproducibility of these gene lists, we performed semiquantitative RT-PCR using the same RNA used for microarray analysis. Four randomly selected pairs of cancer and corresponding noncancerous tissue samples were analyzed in 80 randomly selected genes. Concordant results were obtained for four